2012

AN EXPERIMENTAL INVESTIGATION OF THE HEAT TRANSFER CAPABILITY AND THERMAL PERFORMACE OF DUAL LAYER PULSATING HEAT PIPES

Kyle Morris
University of Rhode Island, kylemorris9098@gmail.com

AN EXPERIMENTAL INVESTIGATION OF THE HEAT TRANSFER CAPABILITY AND THERMAL PERFORMACE OF DUAL LAYER PULSATING HEAT PIPES

BY

KYLE MORRIS

A THESIS SUBMITTED IN PARTIAL FULFILLMENT OF THE REQUIREMENTS FOR THE DEGREE OF

MASTERS OF SCIENCE

IN

MECHANICAL ENGINEERING AND APPLIED MECHANICS

UNIVERSITY OF RHODE ISLAND

2012

MASTER OF SCIENCE IN MECHANICAL ENGINEERING AND APPLIED MECHANICS THESIS

OF

KYLE M. MORRIS

APPROVED:

Thesis Committee:

Major Professor Zongqin Zhang

Donna M. L. Meyer

Walter G. Besio

Nasser H. Zawia
DEAN OF THE GRADUATE SCHOOL

UNIVERSITY OF RHODE ISLAND
2012

ABSTRACT

An experimental investigation on pulsating heat pipes with dual-layer and single layer configurations was conducted in order to determine the effect of the heat transfer and overall system performance given a constrained dimensional heat source with a dual-layer arrangement. The dual layer configuration is an assembly of two pulsating heat pipes of equal measurement connected with a cross linking tube, allowing them to operate using the same working fluid. The dual-layer system was compared to the base single-layer system on several different accounts. These included start-up time and temperature, the average/minimum/ and maximum evaporator temperature during steady state operation, the overall heat transfer capability, and the overall thermal resistance of the system. These requirements were reviewed at different fill ratios: 0%, 25%, 75%, and 90%. The dual layer pulsating heat pipe system (DLPHP) attained the lowest thermal resistance of 0.12 ºC/W at a fill ratio of 75%, while also maintaining an average evaporator temperature of 85 degrees Celsius at an input power of 120 Watts. The single layer pulsating effect, however, was attained at 110 degrees Celsius at its most efficient fill ratio of 50% and a thermal resistance of 0.85 ºC/W and input power of 120 Watts. It was concluded that the dual-layer system exposed to the same input power and area achieved an overall increase in performance with respect to start-up time and temperature, showing start-up oscillation temperatures as low as 73 degrees Celsius, compared to the 88 degrees Celsius required to observe temperature oscillation in the single layer pulsating heat-pipe (SLPHP).

ACKNOWLEDGMENTS

I would like to acknowledge my graduate advisor, Professor Zhang, for helping and assisting me through this project. I would also like to acknowledge my mother, grandparents, and family who inspired me to attain my dreams. I would also like to acknowledge my ever-patient girlfriend, for putting up and dealing with me this year.

TABLE OF CONTENTS

LIST OF TABLES

TABLE PAGE

LIST OF FIGURES

NOMENCLATURE

SLPHP – Single Layer Pulsating Heat Pipe

DLPHP – Dual Layer Pulsating Heat Pipe

D - Diameter (m)

g - Gravitational acceleration (m/s^2)

P - Electrical Power (W)

Q - Heat Transfer Rate (W)

R_{th} - Thermal Resistance (C°/W)

R - Electrical Resistance (Ω)

T - Temperature (°C)

V - Voltage (V)

σ - Surface Tension (N/m)

ρ - Density (kg/m^3)

T_e - Temperature of Evaporator

T_c - Temperature of Condenser

mdot - mass flow rate (ml/sec)

ν - Vapor

l - Liquid

n: Number of Turns.

d_i: Inner diameter of copper tubing.

l_1: Distance of center point of bend from end of copper plate.

R_m: The mean radial distance of the tube bend.

l_e: Total length of copper tube along the copper plate.

CHAPTER 1

INTRODUCTION

In recent years, increasing power levels of electronic components have led to complex thermal dissipation practices. These techniques have had a direct impact on the reliability, performance, and cost of high-performance electronic devices. Current methods rely on heat sink systems, which remove the excess thermal energy through convection and radiation to ambient surroundings [7]. Such heat sink concepts are now designed with intricate cross cut extrusions to increase airflow and convective efficiency [7] [10]. As thermal removal demands increase and current methods are surpassed, new techniques must be investigated.

One alternative method is the relatively new heat transfer system referred to as the Pulsating Heat Pipe (PHP). This heat removal system was chosen for its relative ease of assembly, and its future potential in electronic products that experience high heat dissipation requirements.

In conducted experiments and patent designs, the PHP consisted of a winding tube with a cross-sectional diameter dimension, for which capillary actions of a working fluid may take place [8]. In contrast to a conventional heat pipe, there is no additional capillary structure, such as wicking, inside the tube [1]. This leads to capillary or entrainment performance limitations. Overall, this allows PHP systems to attain higher thermal heat transfer efficiencies over convention heat pipe systems [7].

There have been two proposed ways to assemble the experimental tube structure: closed-loop and open-loop. In a closed-loop design, the tube is joined end-to-end to form a continuous circuit [5], whereas in an open-loop system the tube structure is discontinuous [3]. An illustration in Figure 1 shows a basic orientation and design of a PHP and the schematic of open-loop and closed-loop designs.

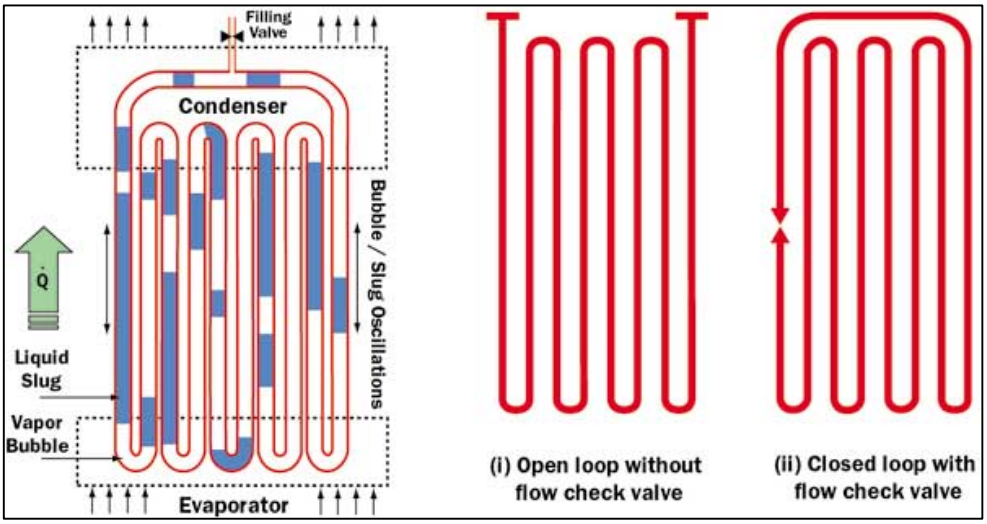

Figure 1: Basic Schematic of Open-loop and Closed-loop PHP

Experiments have been conducted to accurately document the procedures of start-up operations through computer simulation and physical systems [2]. In these trials the tube structure is to first be evacuated to a vacuum and then partially filled with a working fluid. This fluid then distributes itself naturally in the form of liquid-vapor plugs within the capillary tube.

One end of this structure receives heat input from a given source; this end is referred to the evaporator [9]. The heat generated, is subsequently transferred to the opposite end, referred to as the condenser [9]. This is accomplished by a pulsating action first caused by increased vapor pressure of the working fluid in the evaporator. This "pushing" effect causes the liquid-vapor [9] and bubble-slugs throughout the

adiabatic tube sections to be pushed to the condenser. This process allows thermal energy to be released to either a heat sink or ambient surroundings. The condensed working fluid then flows back toward the evaporator [1] and the cycle repeats.

In several PHP experiments, the system is built into a planer surface of a given substrate [5] [6]. Recent research by Khandekar, S. suggests that more turns in the PHP architecture increases the number of perturbations, which is necessary for the pulsating behavior. By adding additional turns to a given design, the heat transfer efficiency is increased [7], however so is the total dimensional foot-print of the design. This can be problematic if the heat source or device for which the PHP is to assist has a dimensional constraint but still requires a particular threshold of thermal dissipation.

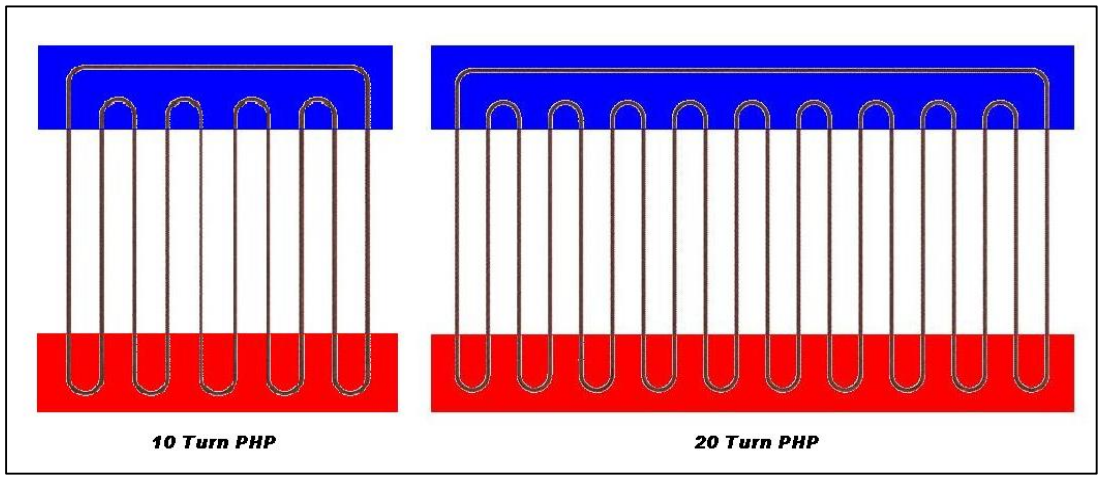

Figure 2: 10 Ten Turn Pulsating Heat Pipe and Twenty Turn Pulsating Heat Pipe

Some researchers have attempted to address this problem by having the tube and turn structures moved closer together, can be seen in Figure 2. This, however, leads to a phenomena referred to as “thermal cross-talk” [5].

“Thermal cross-talk” is defined by the process where heat flows between adjacent flow-channels which can be detrimental to the performance of the device. Too many turns in the system also affect the performance, as friction becomes a

hindrance [11]. The proposed solution to this problem is by reducing the dimensional planar footprint of the device while still maintaining high thermal and heat-flux removal efficiency.

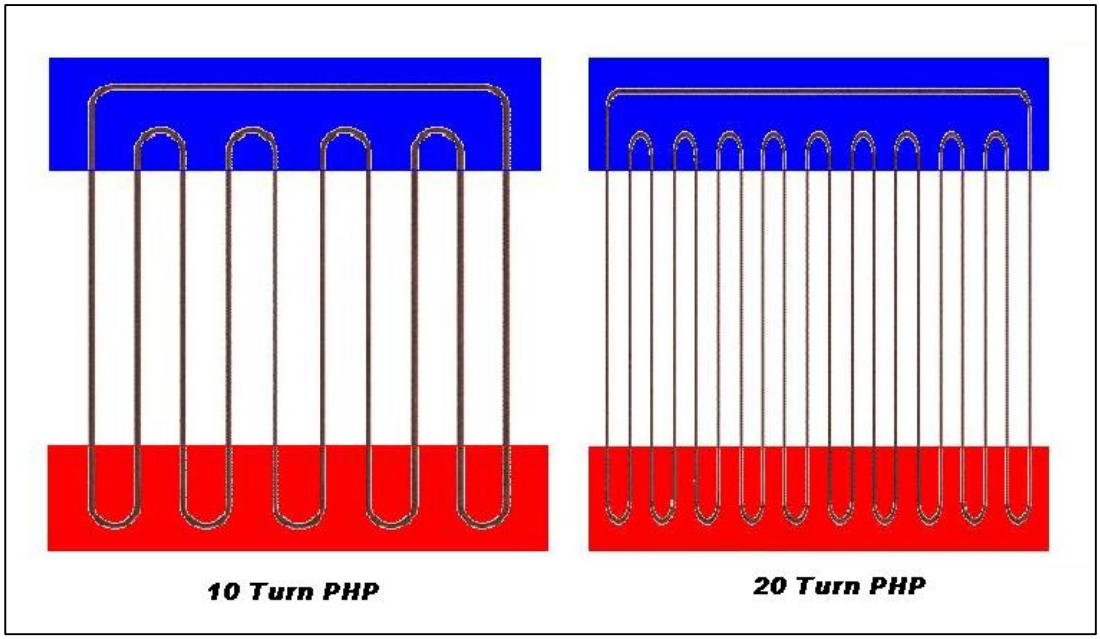

Figure 3: Ten Turn PHP versus Squeezed Twenty Turn PHP

This can be accomplished by connecting two similarly designed pulsating heat pipes in series with each other, while laying one over the other; this concept can be seen in Figure 2 & 3, which will now be referred to as a Dual-Layer Pulsating Heat Pipe. Through this design, it is presumed that for a given dimensional foot print and power density, the heat transfer capacity would double while also retaining the design performance of a larger, continuous, pulsating heat pipe mounted to a dimensionally larger heat source. There is little experimental data or previous research regarding the proposed solution in entailing out-of-plane geometry changes, but it is expected that the system acts similarly to a planar PHP with the same number of turns.

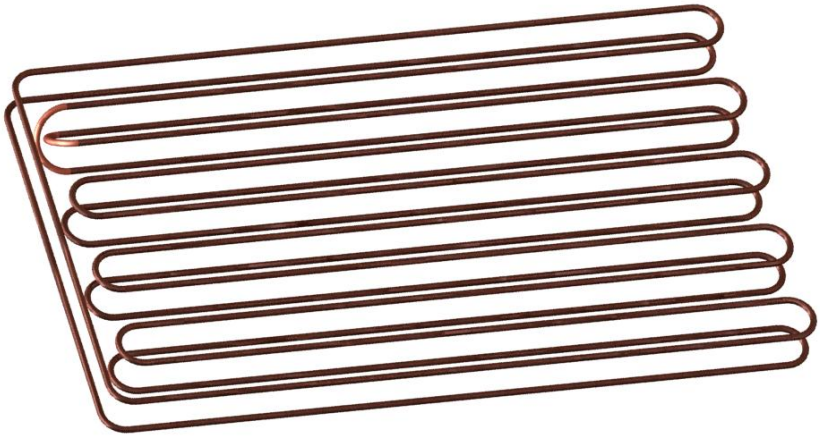

Figure 4: Dual Layer Pulsating Heat Pipe

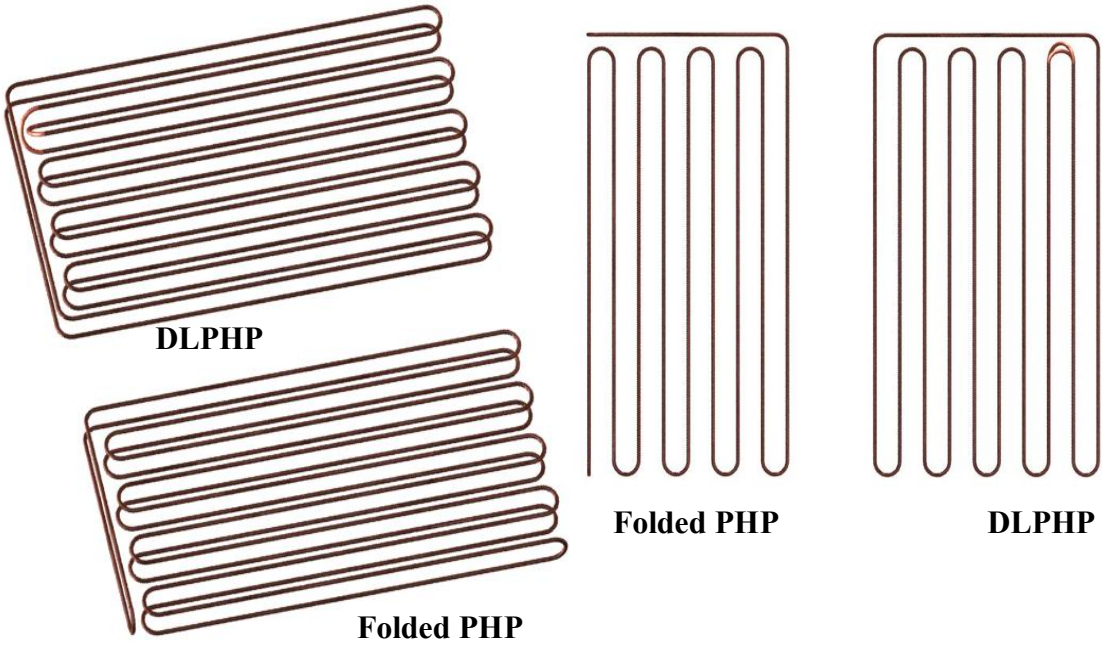

Figure 5: Dual Layer Pulsating Heat Pipe & Potentially Equivalent "Folded" Pulsating Heat Pipe

The study's importance to the advancement of knowledge and its significance relies on the fact that the world is becoming more reliant on electronic devices. From smart phones and laptops for the average consumer, to server farms and mainframes for industrial applications, the demand for higher performing, compact, and more efficient products is growing exponentially. To keep up with this demand, proper methods and research must be taken into consideration. Pulsating Heat Pipes have the

potential to address heat removal demands of future electronic hardware [1]. Current heat-sink methods will eventually become inadequate [7] and it is safe to assume as manufacturing costs are reduced for PHP systems, its relevance will play a greater role as a heat dissipation system.

CHAPTER 2

2.1 REVIEW OF LITERATURE

In the basic understanding of a pulsating heat pipe it is classified as a complex heat transfer device, under a subcategory of heat pipe devices, which experience strong thermo-hydraulic coupling which govern its performance. Also referred to as a non-equilibrium heat transfer device, the successful performance of the device is dependent on the continuous preservation of the non-equilibrium conditions within the system. The vapor and liquid pulsating condition are fully thermally driven, and because of this there is no need for an external mechanical power source, such as a compressor, to move the working fluid from one point to another.

Experiments have also been performed using check-valve assemblies in the adiabatic sections of the system to channel the flow of the system to one direction as well, also referred to as an oscillating heat pipe, which would negate the pulsating effect and would allow the system to perform more as a thermosyphon [7]. Further research on the effect of a check valve on a PHP will be discussed in the Results Section.

The preceding subsections will describe the parameters that affect and make up the inner workings of a typical pulsating heat pipe, including the choice of working fluid, tube structure selection, filling ratio, and the underlying mechanics of the system, including the heat transfer, thermal resistance, and heat flux capabilities.

2.2 TUBE DIAMETER

A design constraint, that has a significant effect on the performance of a pulsating heat pipe, is the hydraulic diameter. In theory, a larger diameter results in a lower thermal resistance in the tube wall and increases the effective thermal conductivity [7]. There is a theoretical limit for which the diameter is constrained to so the balance between the capillary action of the working fluid and the effect of gravity are kept in check as stated by Akachi and Polasek [4]. The maximum theoretical inner diameter can be defined by the following equation [1]:

$$D_{max} = 2\sqrt{\frac{\sigma}{g(\rho_l - \rho_{vap})}} \quad [1]$$

Where σ, g, and ρ are surface tension, gravitational acceleration, and density of the working fluid.

If the diameter chosen is less than the theoretical maximum acceptable inner diameter then tension forces tend to dominate and stable liquid slugs are formed. When the tube diameter is increased beyond the theoretical maximum acceptable diameter the surface tension is reduced and the working fluid within the system will conform to gravity and the system will stop functioning as a typical pulsating heat pipe, and instead would rather operate as an interconnected array of two-phase thermosyphons [7].

2.3 WORKING FLUID

The selection of the working fluid used in pulsating heat pipes is dependent on a number of variables. The approximate temperature range the system will be exposed to is the most critical in determining the proper working fluid. Using an approximate temperature range of 50 to 150 degrees Celsius in turn means many potential working fluids are possible options. Additional requirements need to be examined as well and are listed below:

- Thermal stability
- Wet-ability
- Reasonable vapor pressure
- Compatibility with heat pipe materials
- High thermal conductivity and latent heat
- Reasonable freezing point
- Low vapor and liquid viscosities

For this experiment and various other experiments involving pulsating and oscillating heat pipes, distilled water is used as the working fluid. Water was chosen for its thermodynamic attributes that make it more appealing than others, such as methanol. It has a high latent heat of vaporization of 2260 kJ/kg which has the potential to spread significantly more heat with less fluid flow. Latent heat is defined as the heat required to convert a solid into a liquid or vapor, or a liquid into a vapor, without a change in temperature. This characteristic leads to low pressure drops and high power throughput [5]. The latent heat for condensation of water in the

temperature range from -40 degrees Celsius to 40 degrees Celsius can be approximated by using the following empirical cubic function in equation [2]:

$$L_{water}(T) = -0.0000614342T^3 + 0.00158927T^2 - 2.36418T + 2500.79 \text{[J/g]} \quad [2]$$

Where T is temperature, in degrees Celsius.

The specific latent heat, states the amount of energy in the form of heat (Q) required to completely affect a phase change of a unit of mass (m) and is expressed as:

$$L = \frac{Q}{m} \quad [3]$$

Where:

Q- Is the amount of energy released or absorbed during the change of phase of the substance in kJ or BTU.

m- Mass of the substance in kg or lbs.

L- Specific latent heat for a particular substance in kJ-kg_m^{-1} or in BTU-lb_m^{-1}

Waters high thermal conductivity minimizes the change in temperature associated with two-phase flow in PHP. Water is also a substance that is easily handled and is safe to work with in most environments. Another advantage in using water as the working fluid is that water's high surface tension allows it to generate a large capillary force and allows the pulsating heat pipe to potential operate in many orientations. A potential drawback to this high surface tension is the possibility of causing additional friction and hampering the two-phase flow oscillations.

2.4 WORKING FLUID FILLING RATIO

Another critical parameter which affects the performance of a pulsating heat pipe is the fill ratio of the working fluid. The fill ratio is defined as a percentage of the total inner volume of the system. There has been significant research already performed on the operational limits of a Pulsating Heat Pipe and how it is affected by the fill ratio. The following will describe some of the characteristics of a PHP at different filling ratios.

At a 0% filling ratio, which means no working fluid is present, a heat pipe system behaves as a pure conduction mode heat transfer device [7]. This scenario of bare tubes generates a very high undesirable thermal resistance. The theoretical model for determining the performance of a PHP at 0% fill ratio would be to calculate the heat transfer across a length of pipe and the pipes cylindrical wall.

At a 100% filled heat pipe system the operation observed is similar to a single-phase thermosyphon. In this situation the desired pulsating effect is nonexistent, however studies have been performed that have shown substantial heat can be transferred due to liquid circulation in the tubes by thermally induced buoyancy. The thermosyphon action can be maximized in a vertical heat pipe and stops for a horizontal heat pipe and heat transfer takes place purely by axial conduction. [7] A simple schematic of a closed single loop single-phase thermosyphon can be seen below in Figure 6.

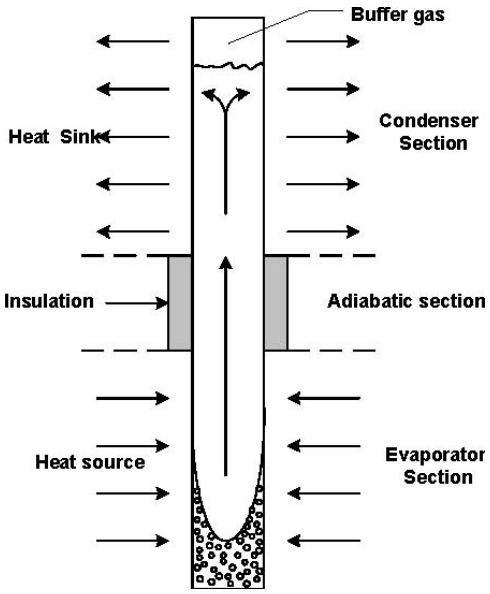

Figure 6: Schematic of Closed Single Loop Single-Phase Thermosyphon

To achieve the ideal performance of a Pulsating Heat Pipe a logical approach is to introduce a two-phase flow system instead of a single phase arrangement. This can be attained by partially filling the PHP with a working fluid to an ideal percentage of volume, which will be discussed in detail further in the text. By partial filling, the system a latent heat advantage due to the evaporation and condensation of bubbles can be achieved [7]. In addition, the temperature gradient between the heater and cooler joined with bubble growth and collapse will generate self-sustaining pressure perturbations. These perturbations cause liquid plug transport and with it, sensible heat transfer. Also because of the introduction of a two-phase system, the pulsating heat pipe has the potential to be orientation independent [4].

Typically pulsating heat pipe fill ratios can be characterized into three distinct operational categories. The first category would be near the 0% filled ratio, in this situation there is very little working fluid to form substantial water slugs, and there is a significant tendency towards an evaporator dry out. In a dry out scenario, the

evaporator will attain undesirable temperatures as the available water slugs and vapor plugs move up to the condenser and remain there. This is caused from the lack of the required vapor pressure, which is insufficient, to transport the working fluid back toward the evaporator. An experimental study of a "dry-out scenario" would show similar results to a 0% fill ratio system, with very little to no fluctuation in the evaporator temperature and very little heat transfer to the condenser, this can be observed in trials performed in the Results Section of this paper.

The second category would be referred to as a system that is at an almost 100% working fluid fill ratio, when with general characteristics of a single phase thermosyphon, but has the negative effect of additional surface tension generated by the friction of the bubbles.

The ideal working range of a Pulsating Heat Pipe is between approximately 20 to 70% filled ratio. Within this range the system performs like an accurate pulsating structure. The ideal range differs for different systems, orientations, working fluids, and operating parameters. This paper investigates the performance of both a single layer pulsating heat pipe and a dual layer pulsating heat pipe, at various fill ratios: 0%, 25%, 50%, 75%, and 90% while using the same watt density in the evaporator section and power input.

2.5 HEAT TRANSFER CAPACITY

The heat transfer capacity of a typical pulsating heat pipe can be calculated using equation [4]:

$$Q = \frac{\Delta T}{2R_{wall} + R_{evp} + R_{1-v} + R_{cond}} = \frac{\Delta T}{\frac{L_{eff}}{k_{eff} * A_{cross}}} \qquad [4]$$

Where ΔT is the overall temperature difference along the heat pipe; k_{eff} and L_{eff} are the effective thermal conductivity and length, and A_{cross} is the cross sectional area of the pulsating heat pipe.

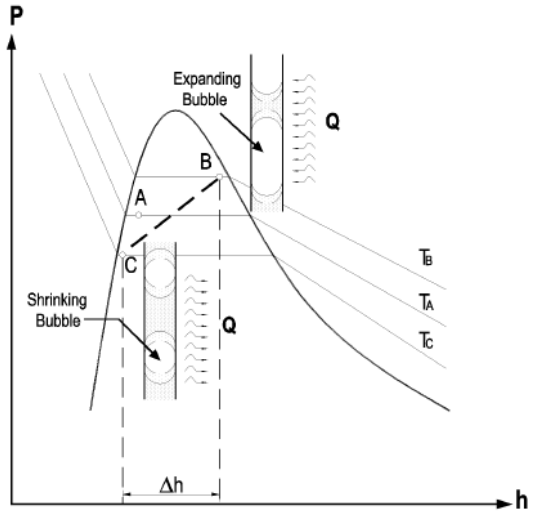

Figure 7: Pressure Enthalpy (P-h) Diagram of a Pulsating Heat Pipe

A pulsating heat pipe that is properly designed and constructed should experience little thermal contact resistance. The conductive thermal resistance in the wall can also be considered negligible. The contact and conductive resistances are independent of the heat pipe operating temperatures, and because of this the thermal resistances due to the evaporation in the evaporator, R_{evp}. Two-phase flow along the

heat pipe, R_{l-v} and the condensation in the condenser, R_{cond} are, however, significant to the performance of the heat pipe.

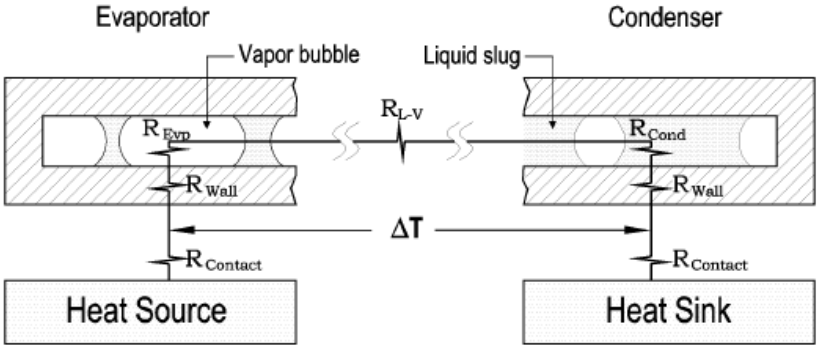

Figure 8: Thermal Resistance schematic of a typical pulsating heat pipe

Typically during operation of the PHP, a continuous flow boiling associated with strong bubble growth and water slug flow takes place in the evaporator section of the heat pipe. The two phase flow continues its way towards the heat pipe condenser section where the bubbles collapse and condense while giving up their latent heat of vaporization.

The vapor-liquid thermal resistance through the length of the pulsating heat pipe R_{l-v} is a function of the temperature and pressure drop from the evaporator to the condenser. Typical pulsating heat pipes in previous studies have shown small thermal resistances, ranging from $(3.29 \times 10^{4}$ /A)/°C/W and $(2.10 \times 10^{-3}$/A) /°C/W. [7]

2.6 REVIEW OF ASSUMPTIONS

As discussed above there are many parameters and design criteria that must be taken into consideration when producing and analyzing a pulsating heat pipe. Along with these criteria some general assumptions must be made to simplify the complex two phase vapor/liquid system that is a pulsating heat pipe.

In review, the flow pattern in a typical pulsating heat pipe can be categorized as capillary slug flow. The characteristics of the flow pattern are axis-symmetric, and the velocity of large vapor bubbles relative to the liquid slug is relatively slow. Also due to the capillary dimensions of the pulsating tube, the liquid plugs are usually characterized as developing a meniscus on the water plug edges [3]. In addition, previous research has also shown a liquid thin film may also exist surrounding the vapor plug.

The major contribution of pressure drop in a capillary slug flow comes from the liquid plug bubble, and the in between length of the bubble body does not generally contribute to the overall pressure drop [6].

In addition, the liquid and vapor plugs and slugs are subjected to the pressure forces from the adjoining plugs. While the plugs experience internal viscous dissipation as well they also experience wall shear stress as they move in the inner diameter tube structure. Even as the surface tension forces predominate, the liquid and vapor plugs move against the gravity vector, in the direction of the vector or at an angle to it depending on the pulsating heat pipes orientation. [3]

Another assumption and observation that has been previously studied is that the liquid-vapor slugs may obtain heat, discard heat or shift without any outside heat

transfer depending on their location in the condenser, the evaporator, or the adiabatic section.

In the evaporator, heat is transferred to the liquid plug which is soon followed by evaporation transfer of mass to the adjoining vapor slug, or even breaks up the liquid slug and creates new bubbles in between as a result of nucleate boiling in the slug flow regime [7]. This process previously mentioned is repeated in the reverse order of operation for the condenser.

An additional observation is related to the adiabatic section of the device. In this section as the working fluid passes from the condenser to the evaporator or vice-versa the train of vapor-liquid slug and plugs are subjected to a series of complex heat and mass transfer processes. This means that non-equilibrium conditions exist, where high pressure, high temperature saturated liquid-vapor are taken down to low pressure, low temperature saturated conditions. In a system with no axial conduction of heat through the tube wall and the fluid itself – meaning adiabatic conditions are maintained – then an irreversible isenthalpic process, which assumes that the process takes place from initiation to completion without an increase or decrease in the entropy of the system, can be accomplished [4].

Also an interesting observation by Khandekar states there is no “classical steady state” in Pulsating Heat Pipe operation. He continues by stating that instead of this, pressure waves and pulsations are generated in each of the individual tubes which interact with each other possibly generating secondary and ternary reflections with perturbations. [4]

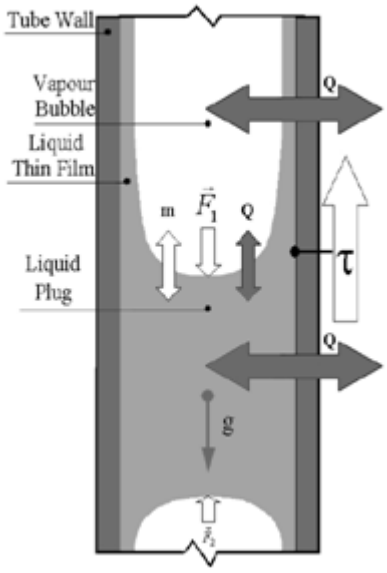

Figure 9: Transport Processes in a Pulsating Heat Pipe

CHAPTER 3

METHODOLOGY

Throughout the research study, many methods were approached to assemble a working and testable pulsating heat pipe system for which to compare results to the dual layer PHP. Each method produced its own manufacturing challenges. As each of these difficulties was resolved, the construction process was refined and a working solution was later found.

The reasoning behind the excessive prototype development and design phase was due to the lack of manufacturing information available for pulsating heat pipes for which the inner mechanisms of the working fluid action could be observed through glass tubing. The majority of research studies performed in this area had access to x-ray type machines that could observe and record the working fluid in action in an enclosed tube structure. For this thesis, which did not have access to such technology, another method for visualization had to be developed.

3.1 PROTOTYPE I

The original proposed design, seen in Figure 8, was to etch a serpentine channel pattern onto a block of clear acrylic, and at a later date, a panel of aluminum. This pattern would then be sealed off, so a working fluid could be injected into the vacant volume. One side of the system was to have an indented location for a strip heater, and the other end of the system was to receive a cooling apparatus of some kind. The assumed benefit of this design was the ease of manufacturing the engraved pattern with the use of a CNC machine.

This concept had some inherent design flaws that were not foreseen during the initial design stage. The assembly process to seal the system closed was not fully developed to prevent the working fluid from leaking across multiple channels or out of the system entirely. This leaking would be detrimental to the performance of the pulsating heat pipe, with adverse effects so detrimental that the system would not perform at all. Another issue that was present with this design was the concept of inserting a heater strip directly on to the acrylic surface. The temperatures required to create the pulsating effect from the evaporator to the condenser exceeded the melting point of the acrylic plastic when it came into direct contact with heater at temperatures of 240 degrees Fahrenheit or greater. Also the adhesive that was used to seal the system was insufficient do to the lack of water, heat, and pressure resistance.

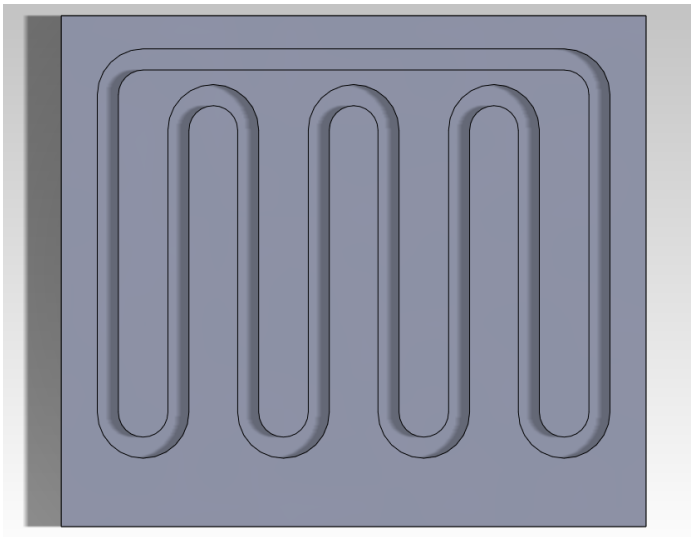

Figure 10: Prototype I Design - Pattern Etched into Substrate

3.2 PROTOTYPE II

After substantial effort and time was put into Prototype I, the idea was abandoned all together and a new design direction, Prototype II, was taken to address many of the previous issues.

The concept of the Prototype II Test Rig, seen under construction in Figure 10, was to address and correct many of the issues presented by Prototype I, which included the working fluid leaking across multiple channels, heat resistance failures, and pressure failures.

Instead of an etched channel pattern in a given substrate that would then require another enclosure on top of the substrate to seal the channel, Prototype II was composed of ¼-inch copper and glass tube segments for visibility.

The two different material tube structures were connected using a heat shrink seal and fiberglass plug, the exploded assembly of this connection can be seen in Figure 9. This approach insured that the material that encountered the strip heater would be able to withstand boiling point temperatures while also withstanding varying high pressure, without forming leaks. This design consideration was used to address the lack of commercial connections for glass to copper tubing of ¼-inch dimensions.

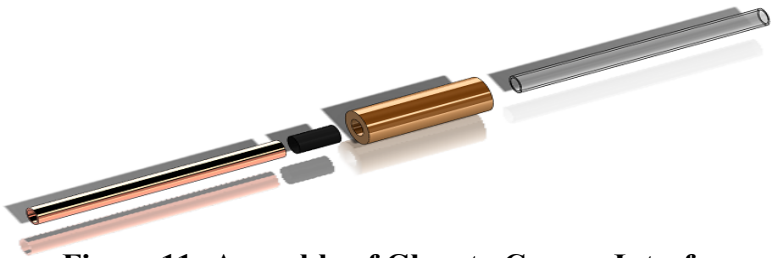

Figure 11: Assembly of Glass to Copper Interface

A more detail-oriented approach was taken to address the assembly of the condenser and evaporator section of the system. The condenser section of Prototype II was composed of a rectangular chamber made out of acrylic plastic. Holes were drilled into one panel of the chamber so the copper sections could be properly inserted. After insertion, a watertight seal around the acrylic and copper tube interface was achieved by using fiberglass resin and harder. Inlet and outlet ports were drilled into the condenser box to allow condenser-cooling fluid to flow over the copper tubing.

The evaporator section was comprised of a 15 inch 500W OMEGA Ceramic Insulated Strip Heater. To reduce the heat loss to the environment the heat strip was placed in an insulated ceramic box.

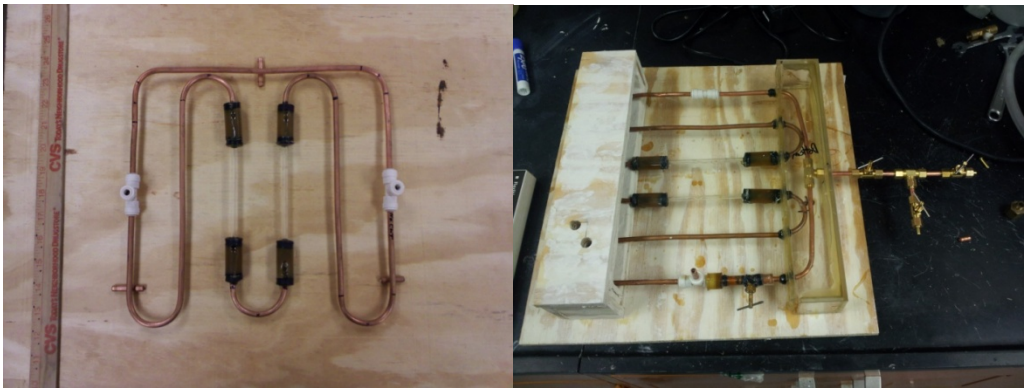

Figure 12: Prototype II Over-View

Preceding tests on this single layer pulsating heat pipe using ¼ inch outer diameter were conducted in the vertical and horizontal orientation at a fill ratio of 50%, using a working fluid of distilled HVAC grade water. During the tests the evaporator temperature was kept at a constant 120 degrees Celsius and the inlet temperature of the condenser was kept at a constant 20 degrees Celsius. During the experiments, several pictures were taken to capture the pulsating flow of the device, which can be seen in Figure 11. After several experiments, it was clear that the

performance of the device was very poor, with very little oscillation. It was determined that the inner diameter of the copper tubing, in respect to the number of turns of the structure, was too large to allow the proper capillary action to take place or the possibility of large vapor plugs to form.

Figure 13: Oscillation of Vapor Slug – Framed at One-Second Intervals

It was concluded from this apparatus and various tests performed with it that to generate a proper pulsating heat pipe, the overall tube diameter would have to be resized to a much smaller diameter, and the number of turns would have to be increased to induce a higher efficiency within the system.

3.3 PROTOTYPE III

As stated previously from Prototype II, a decrease in the inner diameter of the copper tube assembly was required, as well as an increase in the number of turns. With this understanding Prototype III was developed, which used 3.17mm outer diameter HVAC rated copper tubing and a total of 10, 152.4mm long by 2.4mm inner diameter glass tube sections. The glass sections were used for the adiabatic section of the device, so ocillation and pulsating behavior could be visually observed.

The overall purpose of Prototype III, which can be seen in construction and testing phase in Figure 13, was to fully understand how a pulsating heat pipe operates. The purpose of the visual PHP was not to draw actual heat transfer related data as the adiabatic was not properly insulated, because of this, there was apparent heat loss from this section to the surrounding atmosphere.

The overall length of the copper/glass tube structure was 330.2mm and 190.5mm wide. A similar approach to the previous prototypes were used to attach the copper and glass sections as well. The condenser box has the given dimensions of 228.6mm x 101.6mm x 50.8mm.

The evaporator section of the device was comprised of an OMEGA Ceramic Insulated Strip Heater. Model No. HCS-237-240V, with overall dimensions of A: 23 inches (584.2mm), B: 22 inches (558.8mm), and the Heated Length C: 18 inches (457.2mm). The device was rated for 1000W at an input Voltage 220V. The schematic of a typical heater strip can be seen in Figure 12.

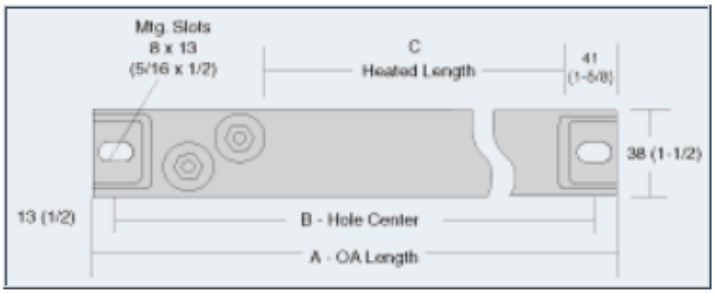

Figure 14: OMEGA Ceramic Strip Heater Schematic

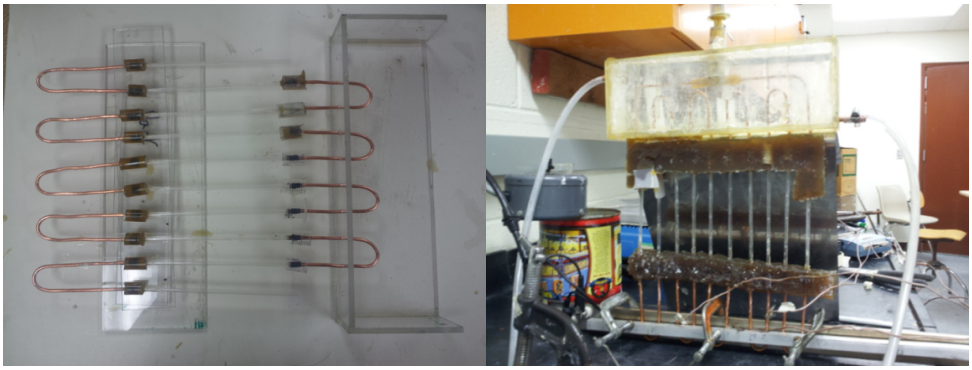

Figure 15: Prototype III Experimental Assembly

Prototype III demonstrated the most promising results, as it showed clear and rapid ocillation in the adabatic sections of the device. A still-picture, which can be seen in Figure 14, was composed with frames from a video that was used to record this ocillation. Figure 14 focuses on one tube, and shows the progression of the water and vapor slug occilation over the period of 2 seconds.

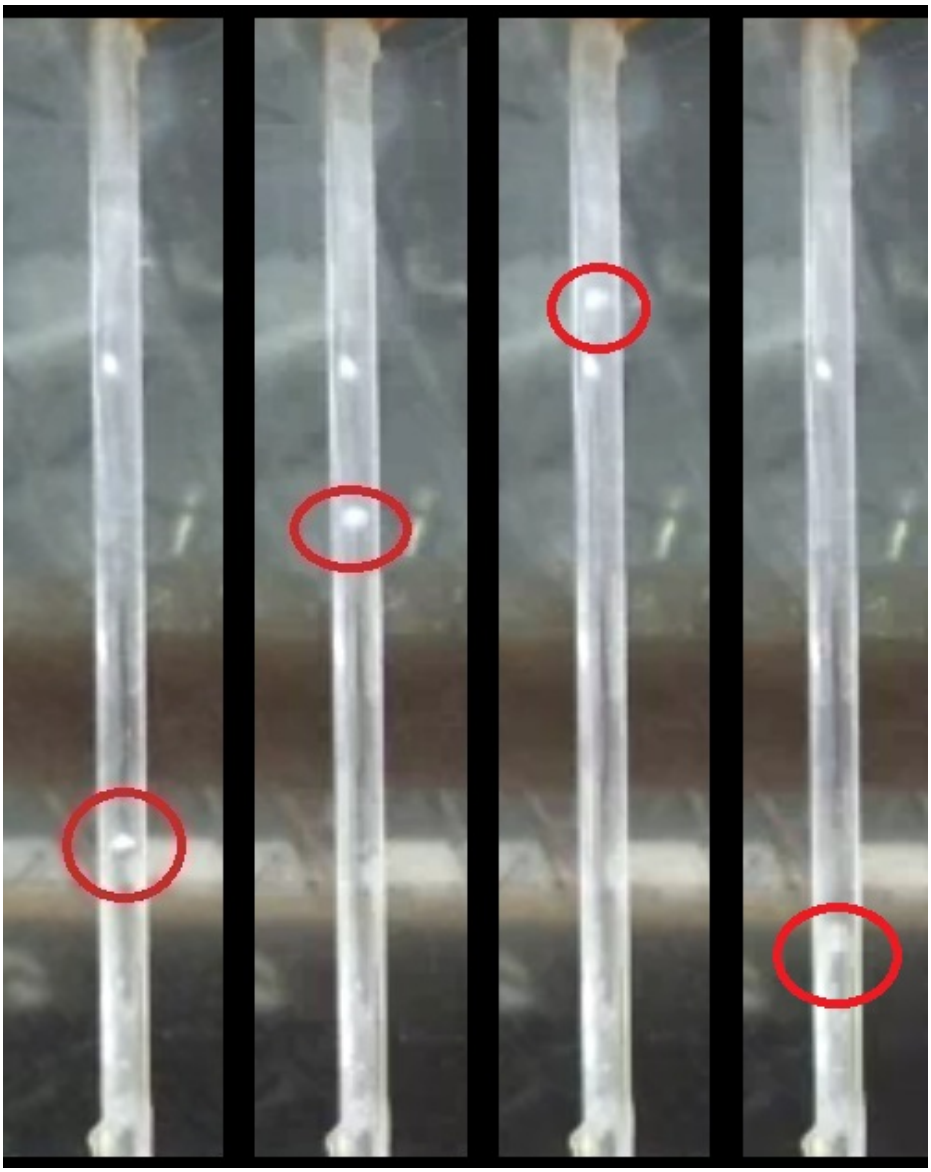

Figure 16: A Frame by Frame Visual of PHP Adiabatic Section

3.4 PROTOTYPE IV

With the success of the Prototype III, a visual dual layer PHP was attempted, with the intention to replicate similar results. A similar construction procedure was used, using the same copper and glass tube structures from Prototype III. Fiberglass resin was used, as the sealant, to connect the glass and copper tube sections. Unfortunately, with the numerous interconnections, proper sealing of these interfaces were not possible, with excessive leaking or pressure loss was evident.

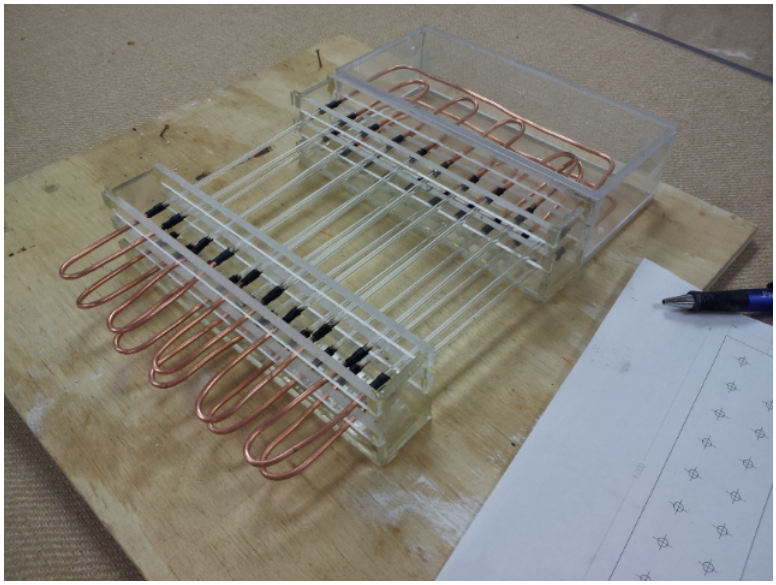

Figure 17: Prototype IV - Visual Dual Layer PHP

3.5 PROTOTYPE V SLPHP and DLPHP

The final design and test rigs, Prototype V: single layer pulsating heat pipe and dual layer pulsating heat pipe, was made completely out of HVAC rated 3.17mm diameter copper tubing. The dual layer system consisted of 18, 180 degree, turns as well as 4, 90 degree bends; the single layer system consisting of 9, 180 degree turns as well as 2, 90 degree bends. The overall length of the copper structure is 330.2 mm, with a width of 155.58 mm. The copper tubes are spaced 22.25 mm from each other, both horizontal and vertically. The copper tubes in the adiabatic section of the device were wrapped in HVAC rated polyethylene pipe insulation at an overall radial thickness of 12.7mm. The thermal conductivity (K) at 75 degrees Fahrenheit (24 degrees Celsius) is 0.03315 W/(m-K). It has an R-valve of 3.582 which is 0.631 $K*m^2/W$. To further reduce the heat loss through the adiabatic section, hot water tank rated fiberglass insulation, with an R-Value of 11, or 1.93721 $K*m^2/W$ was wrapped around the Polyethylene Pipe Insulation as well. Using the below equation [4] the total R-value of the adiabatic section was found to be an R-value of 14.582 or 2.568 $K*m^2/W$.

$$R_{\text{polyethylene insulation}} + R_{\text{fiberglass insulation}} = R_{\text{total}} \qquad [4]$$

The evaporator is composed of a copper plate of thickness 2.54mm, length of 101.6 mm, and a width of 228.6mm. The copper plate and tube structure is soldered with lead-free silver based solder and flux, with a chemical composition of $Sn_{97}Cu_{2.75}Ag_{0.25}$ and a melting temperature of 218 to 314 degrees Celsius based on

application. This type of solder was chosen for its high hardness, creep resistance, as well as its general acceptanace in HVAC and plumbing applications. It is insulated with Hot Water Tank rated Fiberglass Insulation with an R-value of 11, or 1.9372 $K*m^2/W$.

The condenser is composed of acrylic plastic with a length of 101.6mm, a width of 228.6 mm, and a depth of 50.8mm. It is insulated with Hot Water Tank rated Fiberglass Insulation, with an R-valve of 11, or 1.93721 $K*m^2/W$. Computer aided design and actual pictures of the device can be viewed in Figure 16.

Figure 18: Prototype V Dual Layer Pulsating Heat

3.6 METHODOLOGY - EXPERIMENTAL SETUP AND PROCEDURE

The single layer and dual layer pulsating heat pipes were tested using the experimental setup illustrated in Figure 19. This consists of a data acquisition system, with analog to digital converter attached to four thermocouples; this data was acquired and interpreted using a software package referred to as TracerDAQ Pro, which can acquire and plot data from up to 48 channels and acquire up to 1 million samples per channel, also the acquired data can be exported to Microsoft Excel. For this experiment the software was set to record temperature in degrees Celsius with four input channels. The frequency of recording data was set to 2Hz, with each test acquiring up to 7200 individual data points per thermocouple channel for a one hour time span, for a total 28,800 data points per test.

The evaporator section of the device was attached using clamps with an OMEGA Ceramic Insulated Strip Heater. Model No. HCS-237-240V, with overall dimensions of A: 23 inches (584.2mm), B: 22 inches (558.8mm), and the heated length C: 18 inches (457.2mm). The device was rated for $1000W_{avg}$ at an input Voltage $220V_{RMS}$. The schematic of a typical heater strip can be seen in Figure 13. To reduce the thermal resistance between the heater and the copper plate interfaces, OMEGATHERM high temperature and high thermally conductive paste was applied to fill potential gaps. This paste is of thick, grey, and smooth consistancy, and does not harden on long exposure to elevated temperatures; it is rated for continuous use between -40 and 200 degrees Celcius [13]. This paste was also used to mount the thermocouple assemblies to their proper locations.

The strip heater power was regulated with a Powerstate Variable AutoTransformer with 10A fuse. The amount of applied voltage could be adjusted by using this device. For the experiments performed the strip heater was supplied a voltage of $110V_{RMS}$ (Root Mean Square) at an alternating current, which was determined by measurement through a Craftsman Multimeter MPN: 82139, with an accuracy of +/- 1%. The power and watt density of this channel strip heater can be determined by using the following equation supplied by OMEGA Engineering(OEM):

$$Watts\ per\ inch^2 = Wattage/(Heated\ Length\ x\ 3.625) \quad [5]$$

Using the above equation, and using the given data on the applied heater of an average power of $1000W_{avg}$ at $240V_{RMS}$, a watt density of 15.32 watts per $inch^2$ is achieved. Using this information the resistance of the strip heater may be calculated using the following equation:

$$Resistance\ (\Omega) = \frac{Voltage_{RMS}^2}{Power_{avg}} \quad [6]$$

The resistance at the original voltage and power of the heater device is calculated to be:

$$\frac{240V_{RMS}^2}{1000W_{avg}} = 57.6\ \Omega \quad [7]$$

Using a supplied multimeter within the circuit between the powerstat and heat strip, the resistance of the heat strip at $110V_{RMS}$ was also measured to be at 57.6 Ω. Using this information the new power of the strip heater can be calculated as:

$$Power_{avg}(W) = \frac{Voltage_{RMS}{}^2(V)}{Resistance\ (\Omega)} \quad [8]$$

The new power average output of the heater at this voltage is:

$$\frac{110V_{RMS}^2}{57(\Omega)} = 212.28\ Watts \quad [9]$$

For this experiment 10 inches or 254mm of the strip heater will be utilized for the experiment, so a little over half of the available power or approximately 120 Watts will be utilized to heat the system. An overall watt density of 3.24 watts per inch^2 is attained with this voltage input.

The thermal resistance of the entire system can be determined by the following equation:

$$R_{th} = \frac{\Delta T}{Q} \quad [10]$$

Where ΔT is the temperature drop from the evaporator to condenser, and Q is the heat load.

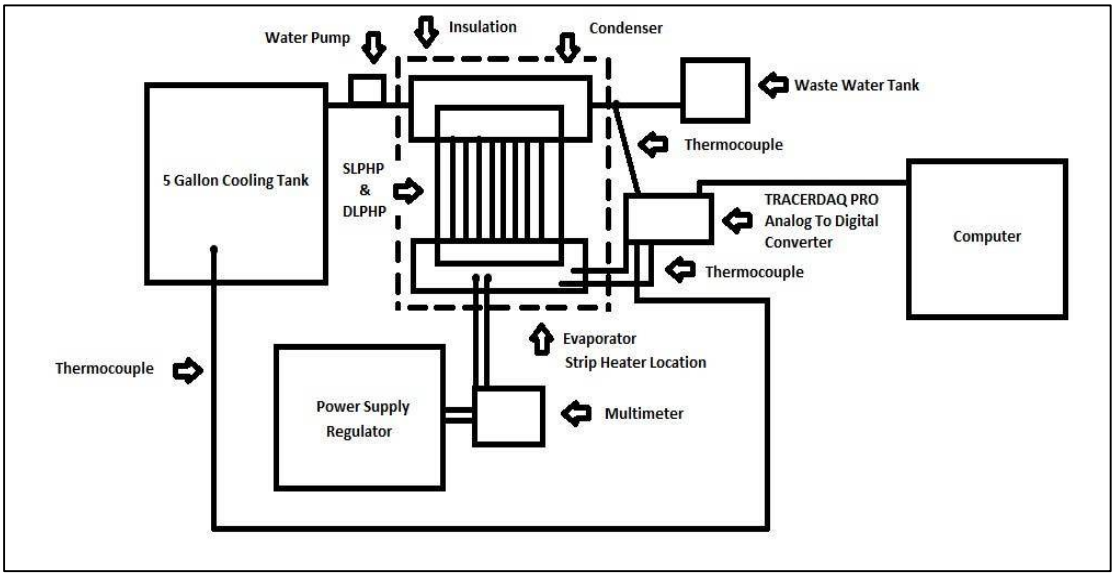

Figure 19: Experimental Setup and Schematic

The condenser section of the experiemental set-up, seen in Figure 17, consisted of a 5 gallon cooling tank that was regulated and kept at a steady temperature of 17 to 18 degrees Celcius. This fluid was then pumped into the condenser box using a Ryobi 2-1/2in Universal Water Pump. This water pump was used to regulate the flow of fluid through the condenser box so proper volumetic and mass flow rates could be determined. The exiting fluid was open to atmosphere and deposited into a waste water tank that was then disposed of. There is some variation in the performance of the cooling tank, due to the system being open to atmosphere, but with a variation of 1 degree Celcius temperature difference throughout the experiments the effects are assumed to neligiable.

The thermocouple assemblies, which have a variation of +/- 0.25°C, were mounted at strategic locations to accurately measure the oscilating and pulsating effects of each system as well as to record the temperature change in the inlet and outlet cooling fluid in the condenser box. On the evaporator section, mounting holes were left in the solder attachments of the copper piping to copper plating so thermocouples could be inserted and come in contact with the piping surface. These mounting holes were then filled with the OMEGATHERM paste to reduce thermal resistance developed at the interface. The remaining thermocouples were placed at given locations on the condenser box assembly. One was placed inside the 5 gallon cooling tank, so temperature could be regulated and monitored. The remaining thermocouple was placed inside the outlet tube of the condenser box assembly. This thermocouple recorded the temperature of the cooling fluid after it has placed through the copper tube assembly. There is some additonal uncertainity in the measured

temperature for the incoming and outgoing fluid due to potential movement on the thermocouple in the fluid path, but the effect is assumed to be negliable.

After the experiment is properly mounted, the cooling fluid is run through the condenser block until a constant and stable mass flow rate is achieved. Then the powerstat, multimeter and strip heater circuit is powered on. The data acquisition software then begins to record temperature data. Several tests were performed on both the single layer and dual layer pulsating heat pipe at various filling ratios. The testing regiment can be viewed in Table 1 and Table 2:

Table 1: Test Schedule for SLPHP at Fill Ratios

Apparatus:	Number of Tests Performed:	Duration of Test (sec)	Cooling Tank Temp	Applied Power	Fill Ratio
SLPHP	3	3600	17-18°C	120W	0%
SLPHP	3	3600	17-18°C	120W	25%
SLPHP	3	7200	17-18°C	120W	50%
SLPHP	3	3600	17-18°C	120W	75%

Table 2: Test Schedule for DLPHP at Fill Ratios

Apparatus:	Number of Tests Performed:	Duration of Test (sec)	Cooling Tank Temp	Applied Voltage	Fill Ratio
DLPHP	3	3600	17-18°C	120W	0%
DLPHP	3	3600	17-18°C	120W	25%
DLPHP	3	7200	17-18°C	120W	50%
DLPHP	3	3600	17-18°C	120W	75%
DLPHP	1	3600	17-18°C	120W	90%

After the above tests are performed the data is analyized using the following equations to view the performance of each device given the various parameters. To determine how much of that heat is transfered to the condenser block another approach and equation has to be used to factor in the potential heat loss through the system.

Using equation:

$$Qdot = \dot{m} * Cp * (Te - Ti) \quad [11]$$

Where:

Qdot: Heat Transfer in (Joules per second).

$\dot{m}$: Mass Flow Rate in (kgs per second).

Cp: Heat Capacity of working fluid (joules/kilogram per kelivn).

Te: Temperature of Exit fluid flow exiting the condenser.

Ti: Temperature of Inlet fluid flow into the condenser.

After this is calculated, the performance of the device can be evaluated by comparing the heat transfer from the heat strip to the condenser temperature. This percentage of performance can be calculated by using:

$$1 - \left(\frac{Qavg.cond}{Qevap}\right) = Percentage\ of\ Heat\ Lost\ Through\ System \quad [12]$$

Where:

$Qcond$: Average Heat Transfer Rate of Condenser at steady state

$Qevap$: Average Heat Transfer Rate of the Evaporator at steady state

The radial and axial heat fluxes in the evaporator section can also be calculated with this information. The radial and axial heat fluxes can be approximated using the following:

$$q_{rad} = Q/A_{rad} \quad [13]$$

$$q_{ax} = Q/A_{ax} \quad [14]$$

Where A_{rad} and A_{ax} can be determined using the following equation.

$$A_{ax} = n * \frac{\pi d_i^2}{4} \quad [15]$$

$$A_{rad} = n * \pi * d_i(l_1 + \frac{1}{2}\pi * R_m) \quad [16]$$

Where:

n: Number of Turns

d_i: Inner diameter of copper tubing

l_1: Distance of center point of bend from end of copper plate

R_m: The mean radial distance of the tube bend

l_e: Total length of copper tube along the copper plate

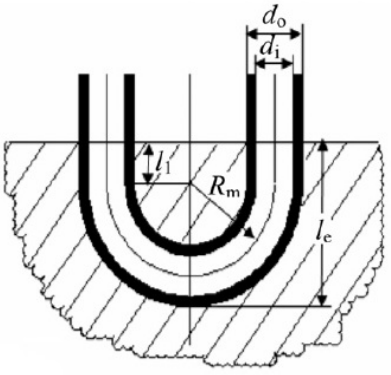

Figure 20: Cross-section Schematic of Evaporator

3.7 SOURCES OF ERROR

A few sources of error were determined during the experiment and trial runs. One potential source of error that could have an impact of the performance of the PHP is the filling ratios. When the systems are charged, the filling ratios are dependent on the calculated inner volume of each tube structure; the inner diameter was measured using a caliper +/- 0.01mm. The inner diameter was assumed to be constant throughout the tube structure, but this is dependent on the tolerances of manufacturers material processing. The overall length of each system was measured prior to each system being bent into configuration.

With this assumption, a process was determined to reduce the error of the inner volume calculation. Each empty system was first weighed on a scale with an accuracy of +/- 0.5 grams and recorded; this process was reproduced 5 times. Each system was then vacuumed, and backfilled with working fluid until the tube structure was assumed to be 100% filled. Each system was then subsequently reweighed and the value was averaged and a standard deviation was determined. The difference between the empty and full system was assumed to be the amount of working fluid present in the system. Based on this calculation the fill ratio amounts were determined with an overall confidence level of 95%.

Also the power input into the system was measured with a multimeter which measures the Root Mean Square of the Voltage with an accuracy of +/-1% of the actual. The reading was taken five times and a confidence interval of 95% was found.

CHAPTER 4

FINDINGS

4.1 INTRODUCTION

Various experimental investigations were performed to observe the effect of dual layer and single layer pulsating heat pipes given a certain watt density heat source, at various working fluid fill ratios. Addition testing was performed on the SLPHP with a mounted check-valve, at varying orientations and filling ratios. As stated previously each apparatus was mounted in the 90 degree orientation. The reason behind this direction was to observe the pulsating heat pipe at its most efficient orientation.

An evaporator assembly was mounted on the bottom section of each pulsating heat pipe, which consisted of a ceramic strip heater set at a power of 120 Watts at an 110V input. At this voltage setting the heat strip reached an average temperature of 155 degrees Celsius.

To accurately record the temperature of the evaporator, and to reduce the chance of error in the results of the evaporator, two thermocouples were placed at predetermined spots along the copper tubing assembly. To improve the accuracy of the thermocouples and to reduce the thermal resistance of contact, OMEGA High Temperature Thermo Paste was applied to the copper tubing and thermocouple contacts.

The temperature oscillation of each system was recorded for 25%, 50%, 75%, and 90% fill ratios. From the gathered data, the heat transfer, the thermal resistance, the

average/ maximum/ and minimum evaporator temperatures, as well as the start-up temperature and time were determined and is further discussed in the following sections.

4.2 EXPERIMENTAL DATA AND ANALYSIS OF SLPHP

As seen in Figure 21, the experimental data of the single layer pulsating heat pipe with a 0% filling ratio, with three trials, were performed and analyzed. The purpose was to set a baseline of how each system performed in pure mode of conduction. As can be seen in the Figure [] the evaporator reaches a very high temperature of approximately 160°C.

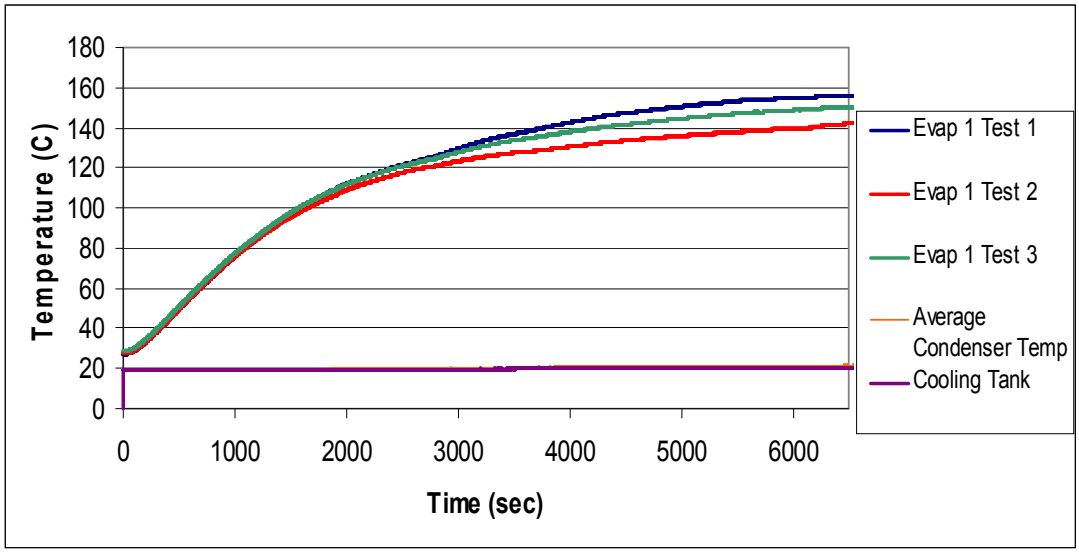

Figure 21: Experimental Data of a SLPHP, at a Fill Ratio of 0%

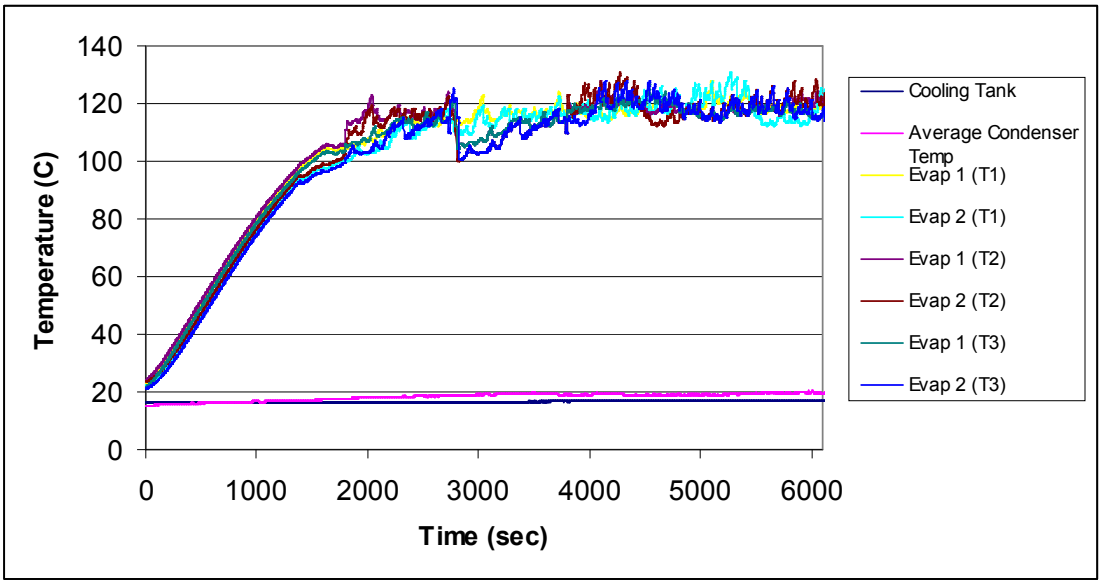

Figure 22: Experimental Data of a SLPHP, at a Fill Ratio of 25%

As seen in Figure 22 the system begins to reach a steady state with a temperature between 110 °C and 120 °C. The system also appears to have a relatively consistent start-up temperature and time, showing an average temperature of 94 °C for Evaporator Thermocouple 1 with respect to the first point of oscillation and 104 °C for Evaporator Thermocouple 2 – this is further detailed in Table 3. The standard deviation, of the data, was 4.16°C during steady state operation.

In addition the temperature oscillation recorded at any one point in time on one tube section on the evaporator, can also be seen affecting the oscillation temperature recorded on a distant tube on the evaporator. This means that the vapor and water plug oscillation in each tube is affecting the fluctuation of other vapor and water plugs throughout the structure, further enhancing the pressure imbalance in the system, as well as preventing the system from reach a dry-out scenario where the evaporator section becomes devoid of working fluid.

Table 3: SLPHP Average Start-Up Time and Temperature

Single Layer PHP Start-Up Time and Temperature			
Fill Ratio (%)	**Time (2Hz)**	**Time (min)**	**Temperature (°C)**
25%	1392	11.6	94
25%	1601	13.34	104

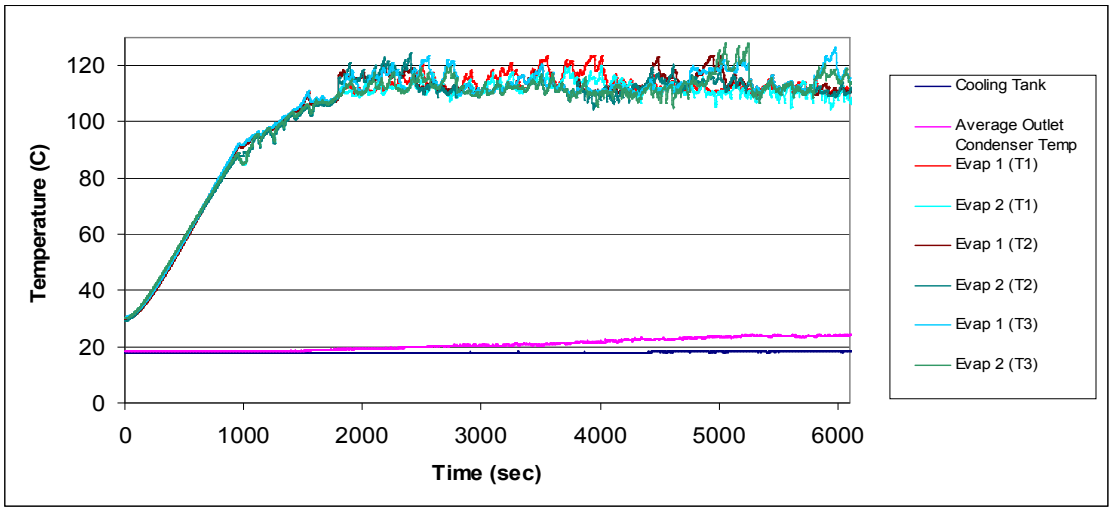

Figure 23: Experimental Data of a SLPHP, at a Fill Ratio of 50%

Figure 23 demonstrates that the system begins to reach a steady state with a temperature range between 110 °C and 120 °C, which is similar to the SLPHP with a 25% fill ratio. The system, with a 50% fill ratio, also appears to have a relatively consistent start-up temperature and time as well throughout all trials, with an average temperature with respect to the first point of oscillation of 88 °C for Evaporator Thermocouple 1 and 93 °C for Evaporator Thermocouple 2 – this is further detailed in Table [4].The Standard Deviation, of the data, was 2.74°C during steady state operation.

Similar to what was discussed concerning the trials involving the SLPHP at 25% fill ratio, the oscillations of temperature at one point in the evaporator tube

structure can be observed affecting the temperature fluctuation at a distance of several tubes away.

Table 4: SLPHP Start-Up Time and Temperature at 50% Fill Ratio

Single Layer PHP Start-Up Time and Temperature			
Fill Ratio (%)	**Time (2Hz)**	**Time (min)**	**Temperature (°C)**
50%	952	7.93	88
50%	965	8.04	93

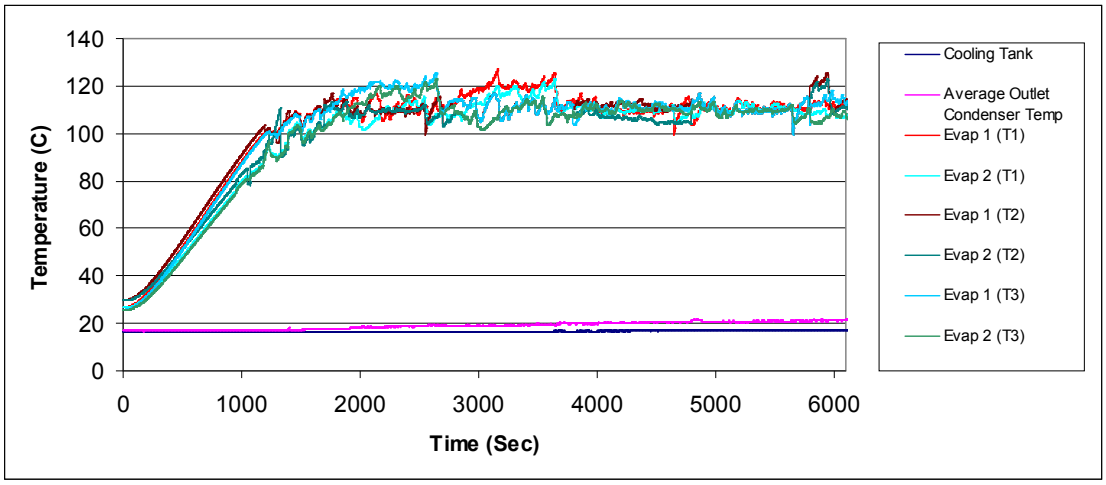

Figure 24: Experimental Data of a SLPHP, at a Fill Ratio of 75%

Figure 24 demonstrates the experimental data of the compiled trials of the SLPHP, with a working fluid of HVAC rated distilled water at a fill ratio of 75%. The system appeared to reach a steady state with a temperature range of 105°C to 120 °C, which shows greater temperature fluctuation within the tube structures. The standard deviation, of the data, was 4.02°C during steady state operation.

The system also appears to have a relatively consistent start-up temperature and time, with an average temperature with respect to the first point of oscillation of 101 °C for Evaporator Thermocouple 1 and 97 °C for Evaporator Thermocouple 2, this is further detailed in Table 5.

Table 5: SLPHP Start-Up Time and Temperature at Fill Ratio 75%

Single Layer PHP Start-Up Time and Temperature			
Fill Ratio (%)	**Time (2Hz)**	**Time (min)**	**Temperature (°C)**
75%	1238	10.31	101
75%	1235	10.29	97

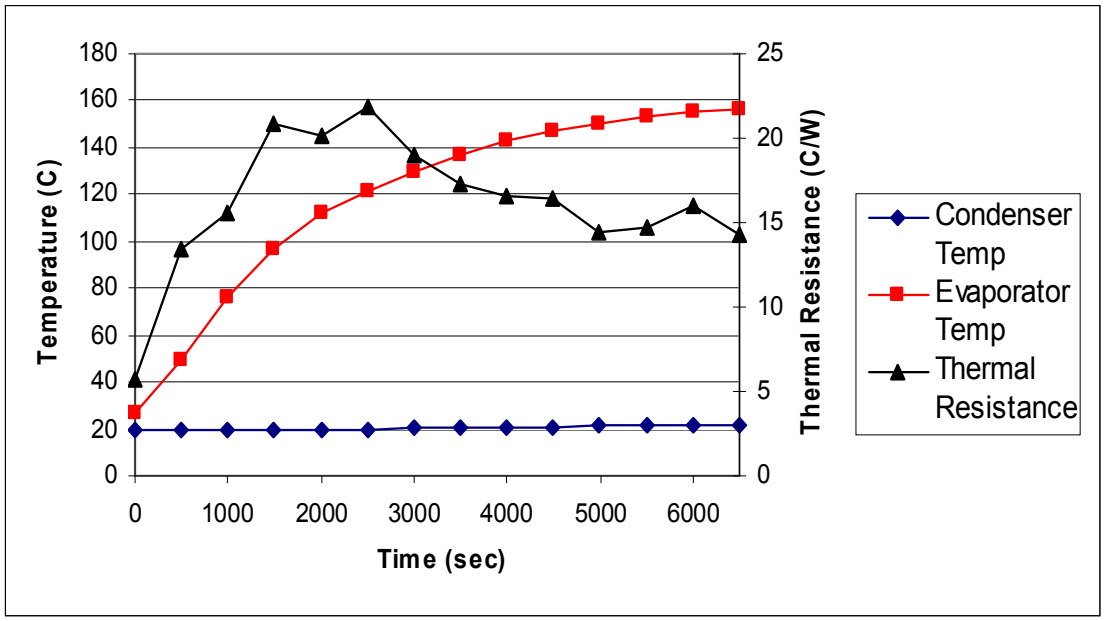

Figure 25: SLPHP with a 0% Fill Ratio Thermal Resistance

Figure 25 shows the thermal resistance of the SLPHP system with respect to time at a working fluid fill ratio of 0%, with data recorded at 500-second intervals. According to the generalized equation [10] previously discussed, the thermal resistance of the system generally peaks at its greatest point during the ramp-up phase of the strip heater power input, and as the evaporator attained a steady state temperature, the thermal resistance begins to drop to an equilibrium state of a 15 °C/W.

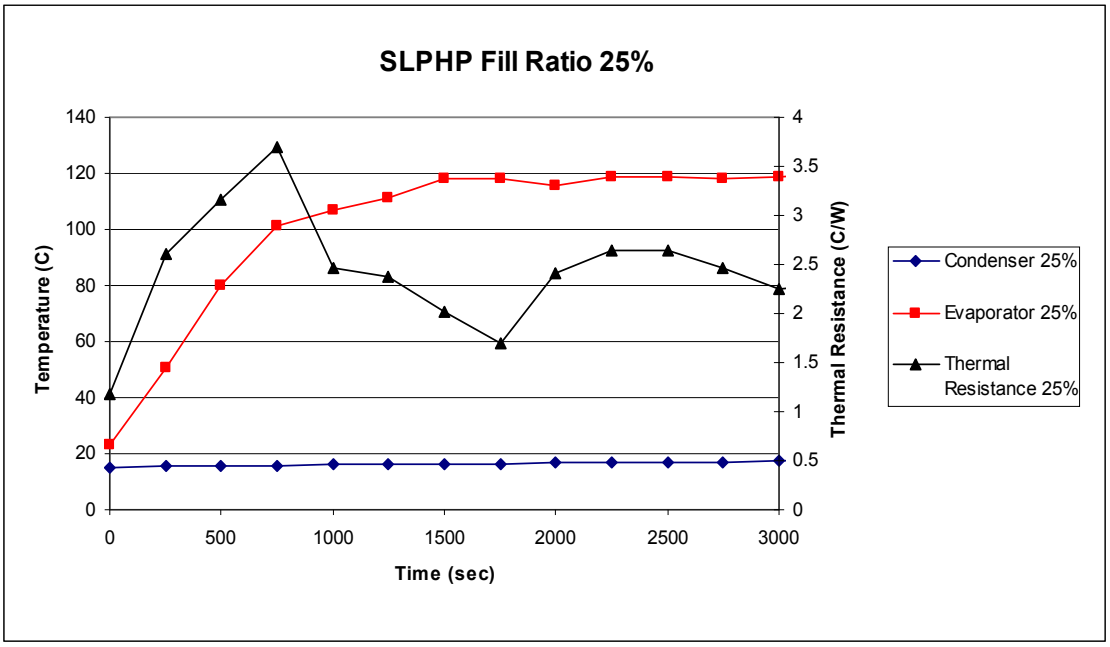

Figure 26: SLPHP with a 25% Fill Ratio Thermal Resistance

Figure 26 shows the thermal resistance of the SLPHP system with respect to time at a working fluid fill ratio of 25%, with data recorded at 500-second intervals. According to the generalized equation [10] previously discussed, the thermal resistance of the system generally peaks at its greatest point during the ramp-up phase of the strip heater power input, and as the evaporator attained a steady state temperature, the thermal resistance begins to drop to an equilibrium state.

For the 25% fill ratio experiment, the maximum thermal resistance of the system was 3.68 °C/W, which peaked as the system began to reach a steady state. The minimum thermal resistance attained during the trial was 1.67 °C/W.

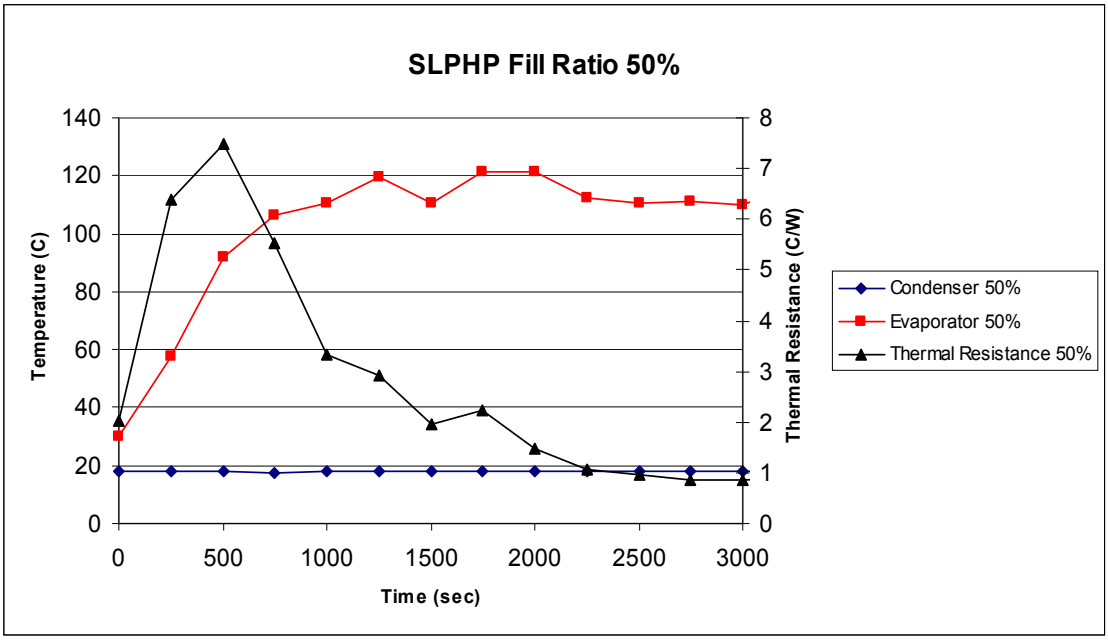

Figure 27: SLPHP with a 50% Fill Ratio Thermal Resistance

Figure 27 shows the thermal resistance of the SLPHP system with respect to time at a working fluid fill ratio of 50%, with data recorded at 500-second intervals. According to the generalized equation [10] previously discussed, the thermal resistance of the system generally peaks at its greatest point during the ramp-up phase of the strip heater power input, and as the evaporator attained a steady state temperature, the thermal resistance begins to drop to an equilibrium state.

For the 50% fill ratio experiment, the maximum thermal resistance of the system was 7.84 °C/W, which peaked as the system began to reach a steady state. The minimum thermal resistance attained during the trial was 0.85 °C/W. The overall performance of the system at this fill ratio during steady state operation was a significant improvement over the experiment with 25% working fluid fill ratio.

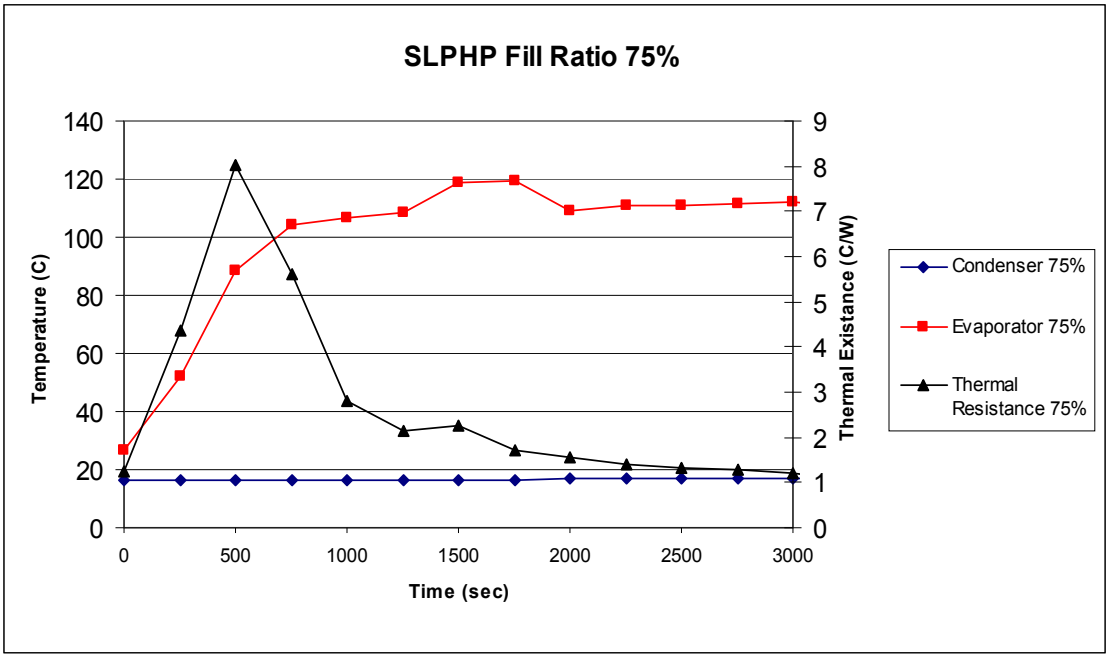

Figure 28: SLPHP with a 75% Fill Ratio Thermal Resistance

Figure 28 shows the thermal resistance of the SLPHP system with respect to time at a working fluid fill ratio of 75%, with data recorded at 500-second intervals. According to the generalized equation [10], the thermal resistance of the system generally peaks at its greatest point during the ramp-up phase of the strip heater power input, and as the evaporator attained a steady state temperature, the thermal resistance begins to drop to an equilibrium state.

For the 75% fill ratio experiment, the maximum thermal resistance of the system was 8.02 °C/W, which peaked as the system began to reach a steady state. The minimum thermal resistance attained during the trial was 1.18 °C/W. The overall performance of the system at this fill ratio during steady state operation was a significant improvement over the experiment with 25% working fluid fill ratio.

4.3 EXPERIMENTAL DATA AND ANALYSIS OF DLPHP

Figure 29 below shows the experimental data of the dual layer pulsating heat pipe with a 0% filling ratio, with three trials performed. The purpose of performing the experiments with zero working fluid is to set a baseline of how each system perform as a pure mode of conduction. As can be seen in the Figure [] the evaporator reaches a very high temperature of approximately 160°C.

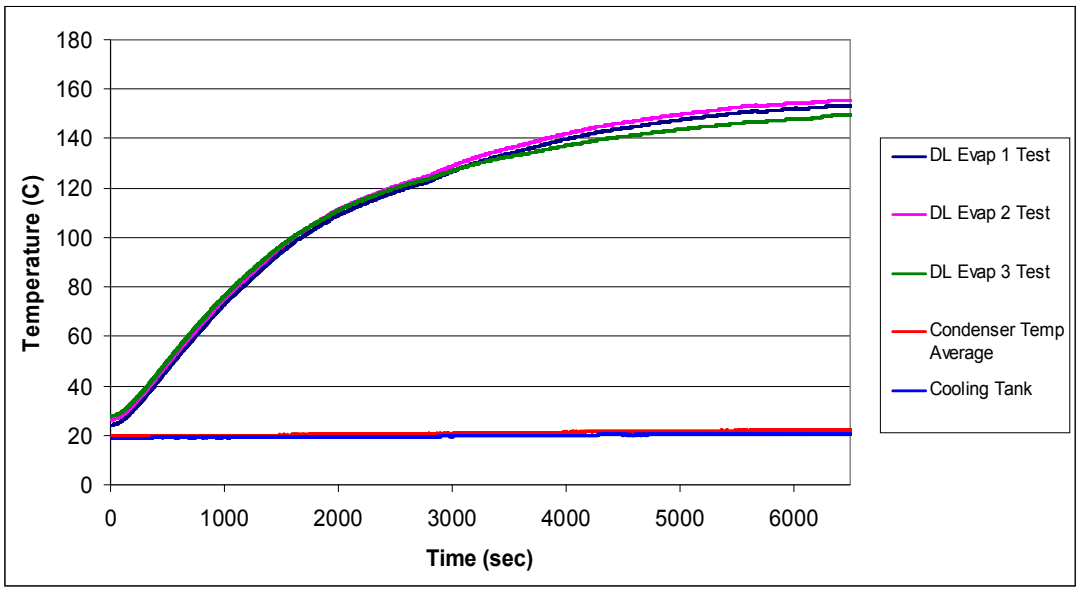

Figure 29: Experimental Data of DLPHP, at Fill Ratio 0%

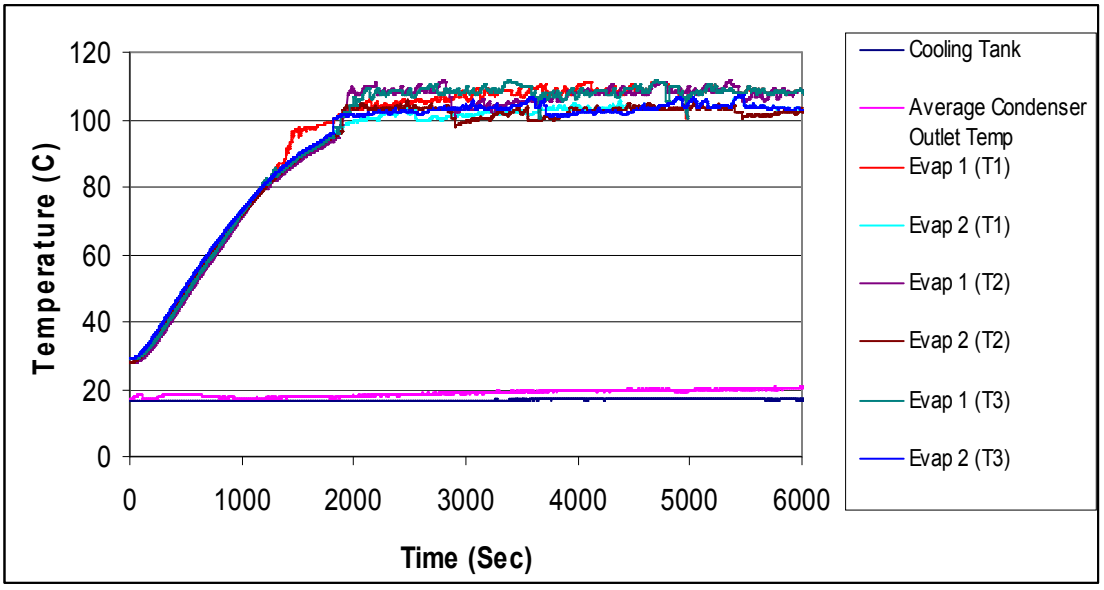

Figure 30: Experimental Data of DLPHP, at Fill Ratio 25%

Figure 30 shows the experimental data of the compiled trials of the DLPHP, with a working fluid of HVAC rated distilled water at a fill ratio of 25%. The evaporator section of the device was allowed to reach a steady state temperature, with an overall temperature range of 100°C to 110°C. An average evaporator temperature of 105°C was maintained during steady state operation. This temperature range was maintained at a lower over all temperature range when compared to ranges attained by the 25%, 50%, and 75% fill ratio trials of the SLPHP. The standard deviation of the above data was 1.7°C during steady state operation.

The system also displayed a relatively consistent start-up temperature and time, with an average temperature with respect to the first point of oscillation of 88 °C for Evaporator Thermocouple 1 and 96 °C for Evaporator Thermocouple 2; further detailed in Table 6. This information is later explained in detail with its significance in respect to the SLPHP configuration.

Table 6: DLPHP Start-Up Time and Temperature with a 25% Fill Ratio

Dual Layer PHP Start-Up Time and Temperature			
Fill Ratio (%)	**Time (2Hz)**	**Time (min)**	**Temperature (°C)**
25%	1700	14.16	88
25%	1822	15.18	96

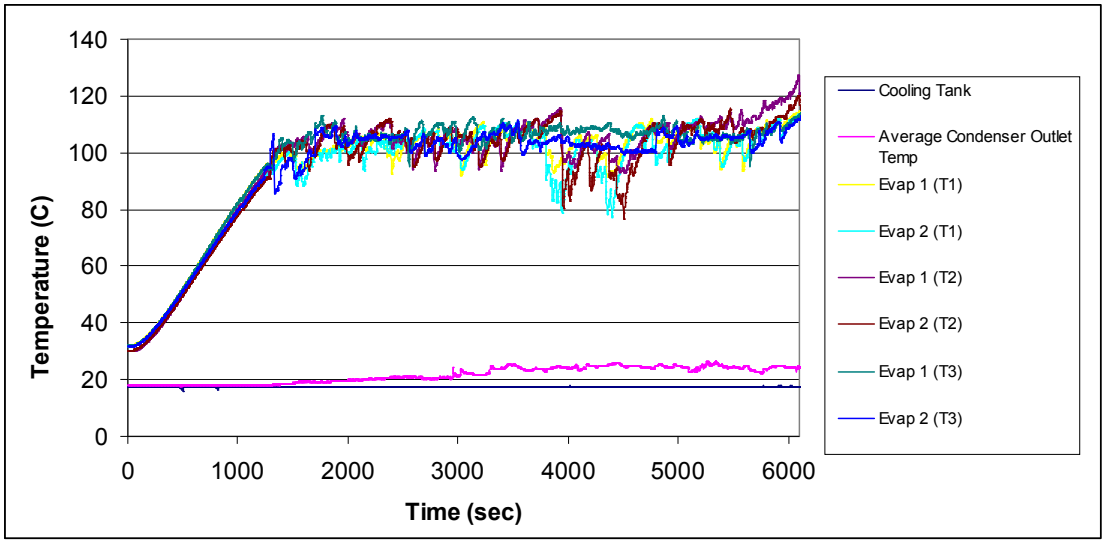

Figure 31: Experimental Data of DLPHP, at Fill Ratio 50%

Figure 31 shows the experimental data of the compiled trials of the DLPHP, with a working fluid of HVAC rated distilled water at a fill ratio of 50%. The evaporator section of the device was allowed to reach a steady state and displayed an oscillation temperature range of 90°C to 110°C. The average temperature of the evaporator during this test was approximately 103°C. The average outlet temperature of the cooling fluid of the condenser during steady state operation was 23°C, which is a 6°C increase of the fluid entering the condenser from the cooling tank. The standard deviation of the above data was 5.45°C during steady state operation.

The system also appears to have a relatively consistent start-up temperature and time, with an average temperature with respect to the first point of oscillation of 81 °C for Evaporator Thermocouple 1 and 84 °C for Evaporator Thermocouple 2, this is further detailed in Table 7.

Table 7: DLPHP Start-Up Time and Temperature with Fill Ratio 50%

Dual Layer PHP Start-Up Time and Temperature			
Fill Ratio (%)	**Time (2Hz)**	**Time (min)**	**Temperature (°C)**
50%	1036	8.63	81
50%	1041	8.67	84

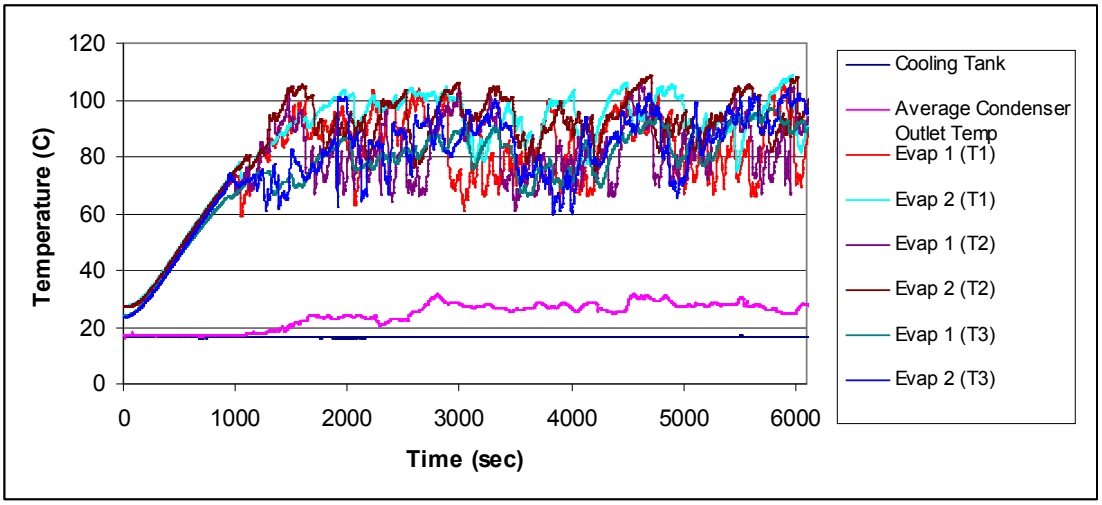

Figure 32: Experimental Data of DLPHP, at Fill Ratio 75%

Figure 32 shows the experimental data of the compiled trials of the DLPHP, with a working fluid of HVAC rated distilled water at a fill ratio of 75%. The evaporator section of the device was allowed to reach a steady state temperature, with a temperature range of approximately 60 °C to 103°C. The compilation of trials, above, show that the most drastic temperature oscillations when compared to trials of both the SLPHP and DLPHP. This which would lead one to conclude that stronger

pressure imbalances are taking place, this goes against the typical performance of a pulsating heat pipe which shows less efficient pulsating or oscillating characteristics as the working fluid percentage approaches 100%. This difference may be do to the construction of the DLPHP, with the possibility that the working fluid did not distribute itself completely between both sections, allowing one section to reach an ideal fill ratio, and the other containing the excess fluid. Another conclusion could be the construction of the DLPHP increased the overall thermal performance range of typical PHP. By placing each section in series, the working fluid from each section worked back and forth from each section. This process allowed each section to attain an ideal fill ratio for a moment, which allowed significant oscillation to occur. It was determined from the results that in order to conclude that the system does not continuously increase in oscillation in respect to higher than 75% fill ratios, an additional test at a higher fill ratio was required.

The system also appears to have a relatively consistent start-up temperature and time, with an average temperature with respect to the first point of oscillation of 73 °C for Evaporator Thermocouple 1 and 78 °C for Evaporator Thermocouple 2, viewed in Table 8. A well as the standard deviation of the above data was 7.24°C during steady state operation. This observation was also of interest as the start-up temperature was significantly less than that of previous trials, for both the SLPHP at all fill ratios as well as the DLPHP with lesser fill ratios. This shows that the system is able to perform at lower operating temperatures when compared to two separate pulsating heat pipes.

Table 8: DLPHP Start-Up Time and Temperature with Fill Ratio 75%

Dual Layer PHP Start-Up Time and Temperature			
Fill Ratio (%)	**Time (2Hz)**	**Time (min)**	**Temperature (°C)**
75%	1000	8.33	73
75%	1041	8.675	78

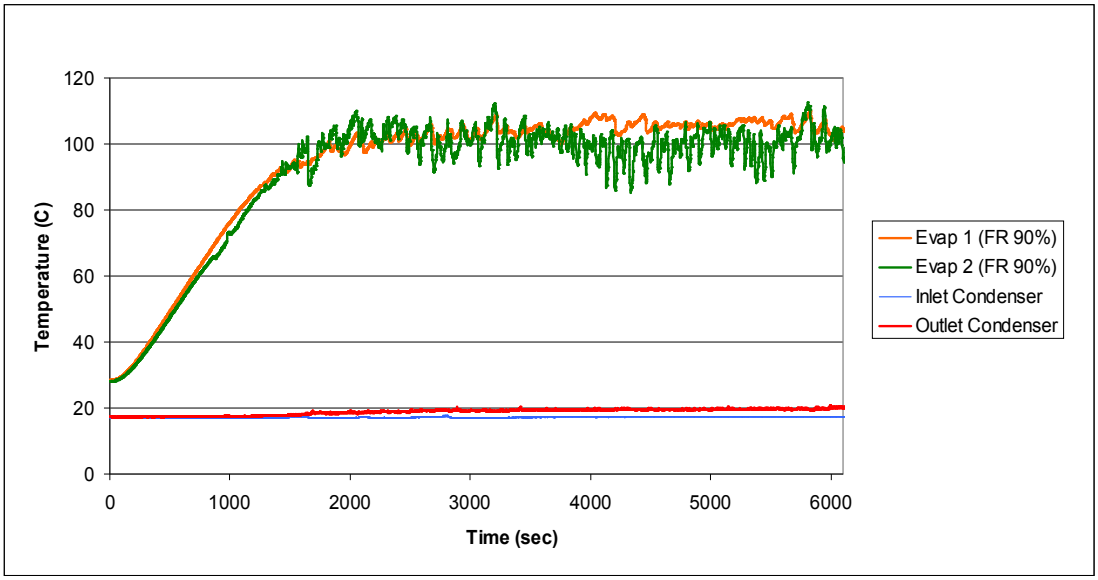

Figure 33: Experimental Data of DLPHP, at Fill Ratio 90%

An additional trial was performed to see if the oscillation and thermal performance of the DLPHP drops off above the 75% fill ratio which originally showed the greatest improvement in thermal management. The DLPHP was charged with distilled HVAC rated water at a fill ratio of 90%. The evaporator section of the device was allowed to reach a steady state temperature and attained an operational range of 90°C to 110°C. This is a significant change in temperature oscillation versus the system charged with a 75% fill ratio.

The system also appears to have a relatively consistent start-up temperature and time, with an average temperature with respect to the first point of oscillation of

92 °C for Evaporator Thermocouple 1 and 89 °C for Evaporator Thermocouple 2, this is further detailed in Table 9.

Table 9: DLPHP Start-Up Time and Temperature at Fill Ratio 90%

Dual Layer PHP Start-Up Time and Temperature			
Fill Ratio (%)	**Time (2Hz)**	**Time (min)**	**Temperature (°C)**
90%	1362	11.35	92
90%	1352	11.26	89

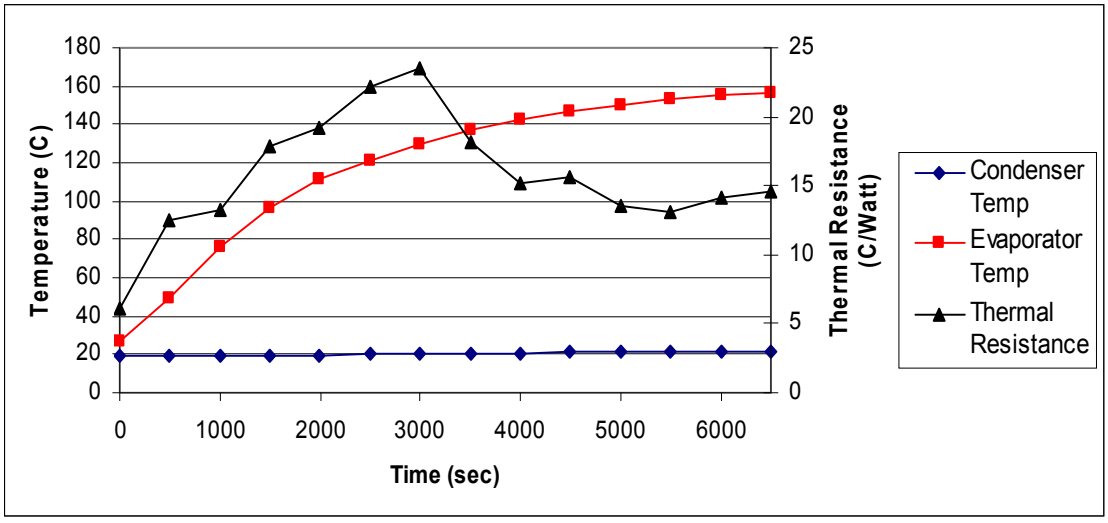

Figure 34: DLPHP with a 0% Fill Ratio, Thermal Resistance

Figure 34 shows the thermal resistance of the DLPHP system with respect to time at a working fluid fill ratio of 0%, with data recorded at 500-second intervals. According to the generalized equation [10] previously discussed, the thermal resistance of the system generally peaks at its greatest point during the ramp-up phase of the strip heater power input, and as the evaporator attained a steady state temperature, the thermal resistance begins to drop to an equilibrium state of approximately 15 °C/W.

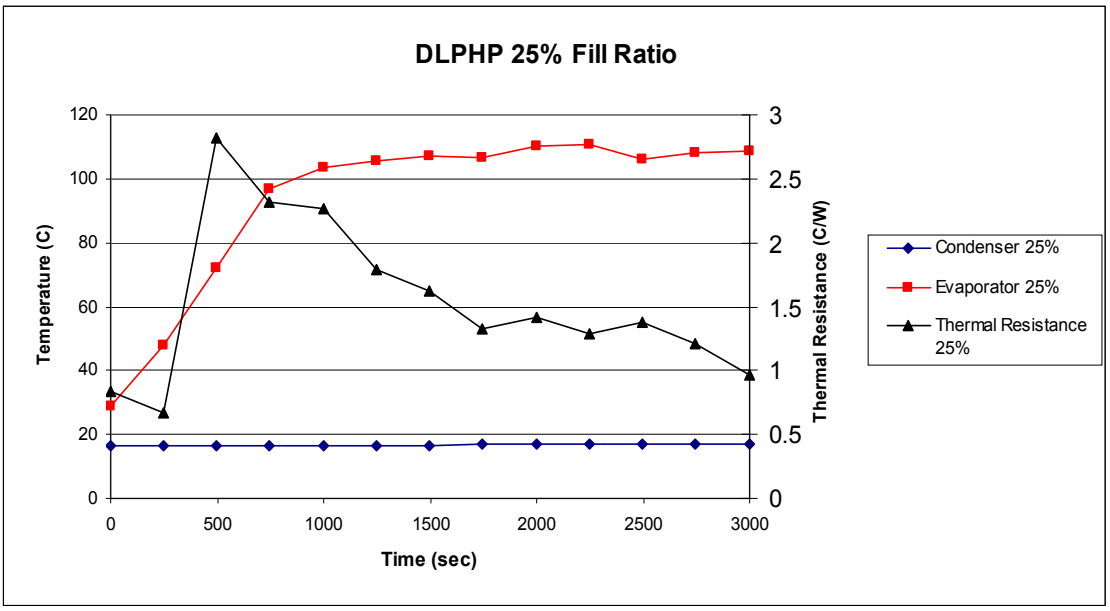

Figure 35: DLPHP with a 25% Fill Ratio, Thermal Resistance

Figure 35 shows the Thermal resistance of the DLPHP system with respect to time at a working fluid fill ratio of 25%, with data recorded at 500 second intervals. According to the generalized equation [10] previously discussed, the thermal resistance of the system generally peaks at its greatest point during the ramp up phase of the strip heater input, and as the evaporator beings to reach a steady state temperature, and the system beings to operate as a heat transfer device the thermal resistance begins to drop to an equilibrium.

For the 25% fill ratio experiment the maximum thermal resistance of the system was 2.81 °C/W with the minimum thermal resistance attained during the trial was 0.96 °C/W. The overall performance of the system at this fill ratio given these thermal resistances can be rated at very poor.

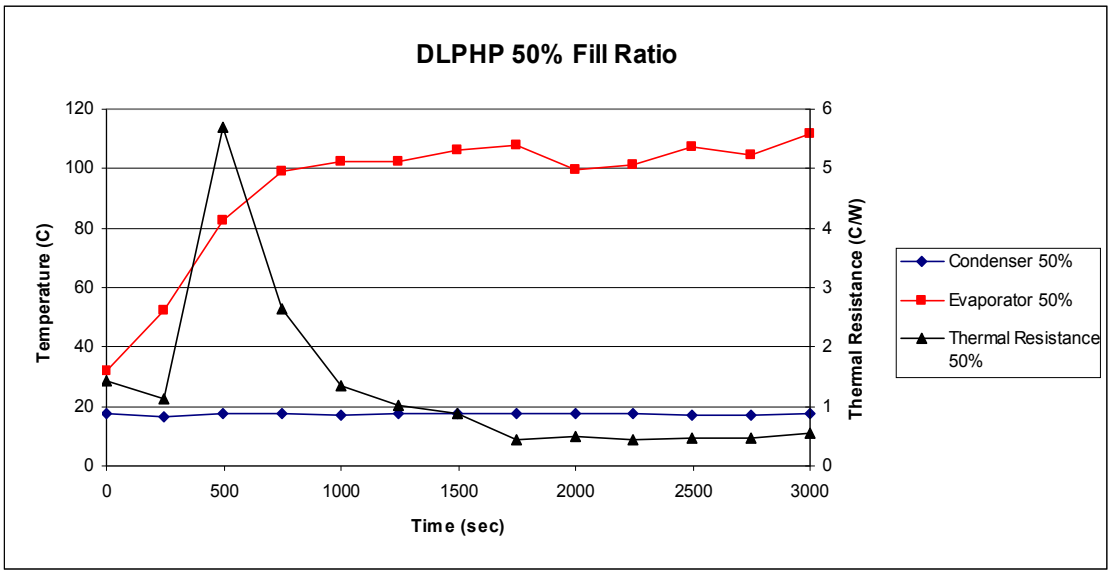

Figure 36: DLPHP with a 50% Fill Ratio, Thermal Resistance

Figure 36 shows the thermal resistance of the DLPHP system with respect to time at a working fluid fill ratio of 50%, with data recorded at 500-second intervals. According to the generalized equation [10] previously discussed, the thermal resistance of the system generally peaks at its greatest point during the ramp up phase of the strip heater input power. As the evaporator attains a steady state temperature and the system beings to operate as a heat transfer device the thermal resistance begins to drop to equilibrium.

For the 50% fill ratio experiment, the maximum thermal resistance of the system was 5.81 °C/W, which peaked as the system began to reach a steady state. The minimum thermal resistance attained during the trial was 0.54 °C/W. The overall performance of the system at this fill ratio during steady state operation was a significant improvement over the experiment with 25% working fluid fill ratio.

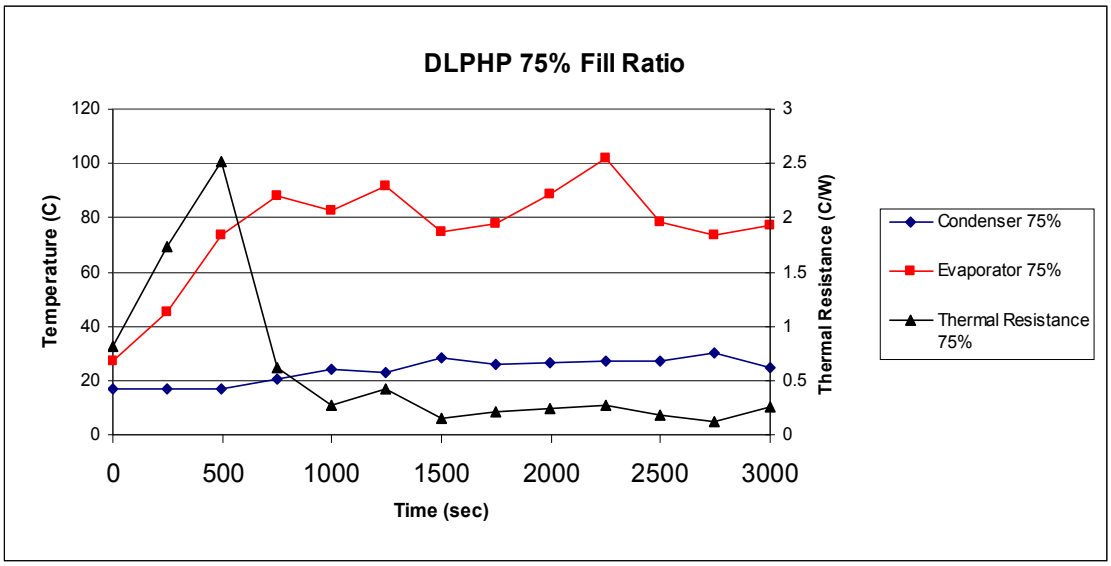

Figure 37: DLPHP with a 75% Fill Ratio, Thermal Resistance

Figure 37 shows the thermal resistance of the DLPHP system with respect to time at a working fluid fill ratio of 75%, with data recorded at 500-second intervals. The thermal resistance of the system generally peaks at its greatest point during the ramp-up phase of the strip heater. As the evaporator attained a steady state temperature, the thermal resistance begins to drop to an equilibrium state.

For the 75% fill ratio experiment, the maximum thermal resistance of the system was 2.52 °C/W, which peaked as the system began to reach a steady state. The minimum thermal resistance attained during the trial was 0.12 °C/W. The overall performance of the system at this fill ratio during steady state operation was a significant improvement over the experiment with 25% working fluid fill ratio.

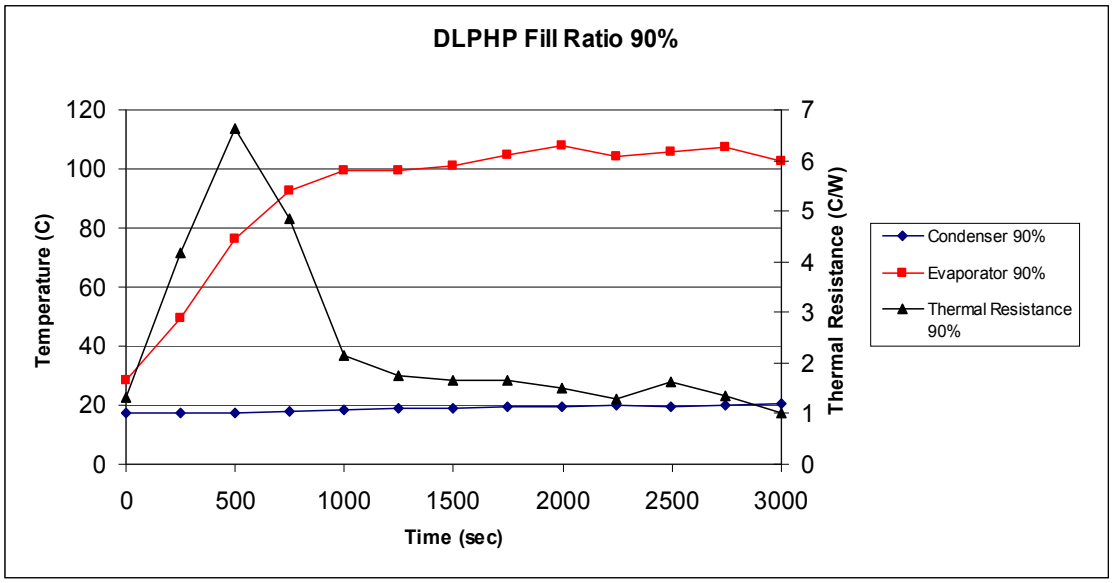

Figure 38: DLPHP with a 90% Fill Ratio, Thermal Resistance

Figure 38 shows the thermal resistance of the DLPHP system with respect to time at a working fluid fill ratio of 90%, with data recorded at 500-second intervals. According to the generalized equation [10] previously discussed, the thermal resistance of the system generally peaks at its greatest point during the ramp-up phase of the strip heater. As the evaporator attained a steady state temperature, the thermal resistance begins to drop to an equilibrium state.

For the 90% fill ratio experiment, the maximum thermal resistance of the system was 6.64 °C/W, which peaked as the system began to reach a steady state. The minimum thermal resistance attained during the trial was 1.05 °C/W. The overall performance of the system at this fill ratio during steady state operation was a significant improvement over the experiment with 25% working fluid fill ratio.

4.4 HEAT TRANSFER AND HEAT FLUX OF SLPHP AND DLPHP

The heat transfer of each system was evaluated using equation [9] in respect to the temperature difference between the evaporator and condenser block, as well as the mass flow rate of the cooling fluid running through the condenser and the heat capacity of the water. The condenser block was wrapped in fiberglass insulation and as so the heat loss out of the condenser tank at any one time is assumed to be negligible. The results of both systems are depicted in Figure 36 and Figure 37.

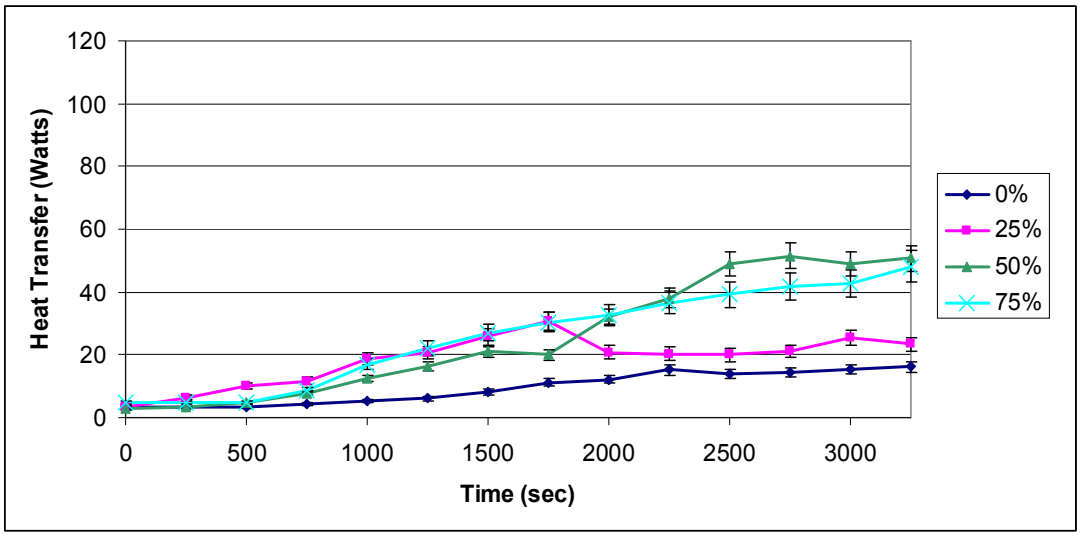

Figure 39: SLPHP Average Heat Transfer to condenser cooling fluid

Figure 39 shows the average heat transfer capacity of the SLPHP system at each fill ratio, the information from each set of trials were averaged and plotted using each data point at 500-second intervals so a consistent and easily observable plot could be generated. A standard deviation of approximately 5 percent at each data point was determined from the averaged data for each set of trials.

The heat transfer, and power transfer, was greatest when the system was charged with a fill ratio of 50%, at approximately 55 joules per second or 55 watts of

power were transferred to the condenser fluid as the system operated at steady state in the evaporator. When compared to the input power of the evaporator of approximately 120 watts the overall efficiency of the system of 45.8%. Meaning approximately 45.8% percent of the evaporator input power was transferred along the system to the condenser.

The worst performance was observed when the system was charged with no working fluid, which achieved an average heat transfer rate of approximately 18 joules per second, or 18 watts during steady state operation, this is from the system operating in means of pure conduction along the copper tubes, and achieved a high relative thermal resistance of 5.83 °C/W.

The system also performed poorly when charged with the 75% and 25% fill ratios following the literature which states that as the fill ratios move toward either 0% or 100% the system produces undesirable results. As the fill ratio approaches 0% the potential for a dry-out scenario increases, where the oscillation of working fluid in one tube structure does not directly affect the working fluid in another tube. As the fill ratio approaches 100%, however, not enough vapor plugs are equally distributed in relation to liquid plugs leading to poor performance from increased surface tension of the liquid plugs [7].

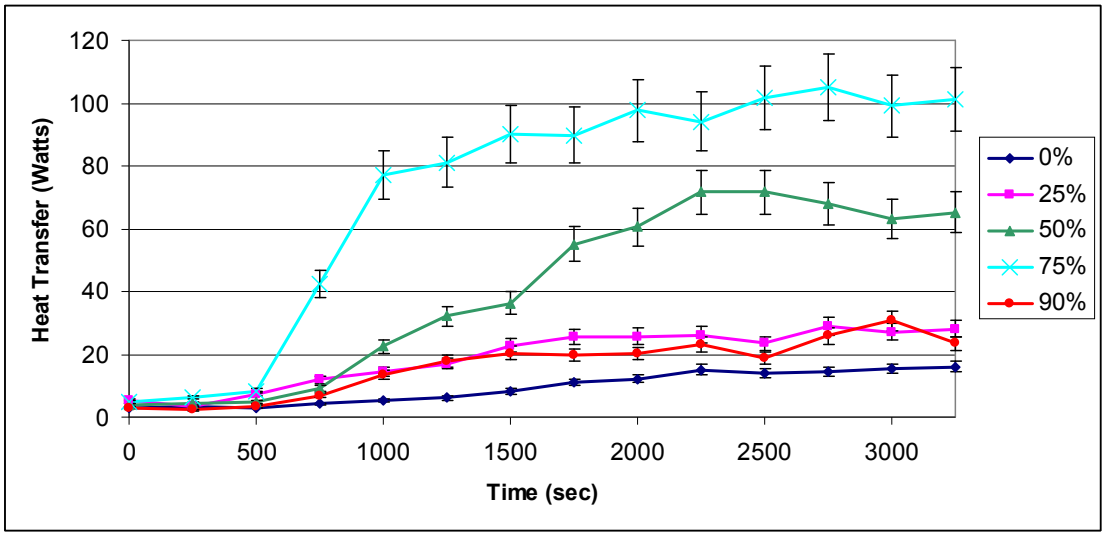

Figure 40: DLPHP Average Heat Transfer to condenser cooling fluid

Figure 40 shows the heat transfer of the DLPHP system at various fill ratios. The heat transfer into the condenser working fluid was calculated using equation [9], which takes into consideration the mass flow rate of the cooling fluid, as well as the inlet and outlet temperature difference of the condenser box, and the heat capacity of the circulating water.

The fill ratio with the highest heat transfer rate was when the system was charged with a 75% fill ratio, attaining an average overall heat transfer rate of approximately 105 joules per second or 105 watts during steady state operation. This is an efficiency of approximately 87.5% when compared to the input evaporator power of 120 watts. This is a substantial increase when compared to the SLPHP at a 75% fill ratio, and because of this observed increase an additional trial was performed with the system charged with a 90% fill ratio which showed a substantial drop off in capacity as a recorded heat transfer rate of 25 watts was attained. The system attained an average heat transfer rate of approximately 65 joules per second or 65 watts, with a

charged filling ratio of 50%. It also appeared to operate poorly with a fill ratio of 25% as well with an average heat transfer capacity of 25 watts.

Table 10: Maximum Radial and Axial Heat Flux in respect to Input Power

	SLPHP	DLPHP
Q_{max} (W)	120W	120W
qax_{max} (W/cm^2)	561	280.6
$qrad_{max}$ (W/cm^2)	5.3	2.65

Using equation [8] the axial and radial heat flux at the maximum heat load were calculated. The SLPHP and DLPHP show similar results, where as the DLPHP was a magnitude of half of the value calculated for the SLPHP, since the DLPHP had twice as many tube structures attached to the evaporator during the test regime with the same input power, this is be expected.

4.5 AVG/MIN/MAX & START UP TIME AND TEMP

As seen in Figure 41 the average temperature of the SLPHP evaporator at steady state, across all fill ratio combinations stayed above an average temperature of 110 degrees Celsius. When compared with SLPHP devoid of working fluid, which attained an average evaporator temperature of 125 degrees Celsius and in parallel with literature there is some temperature regulation advantage given the working fluid fill ratio.

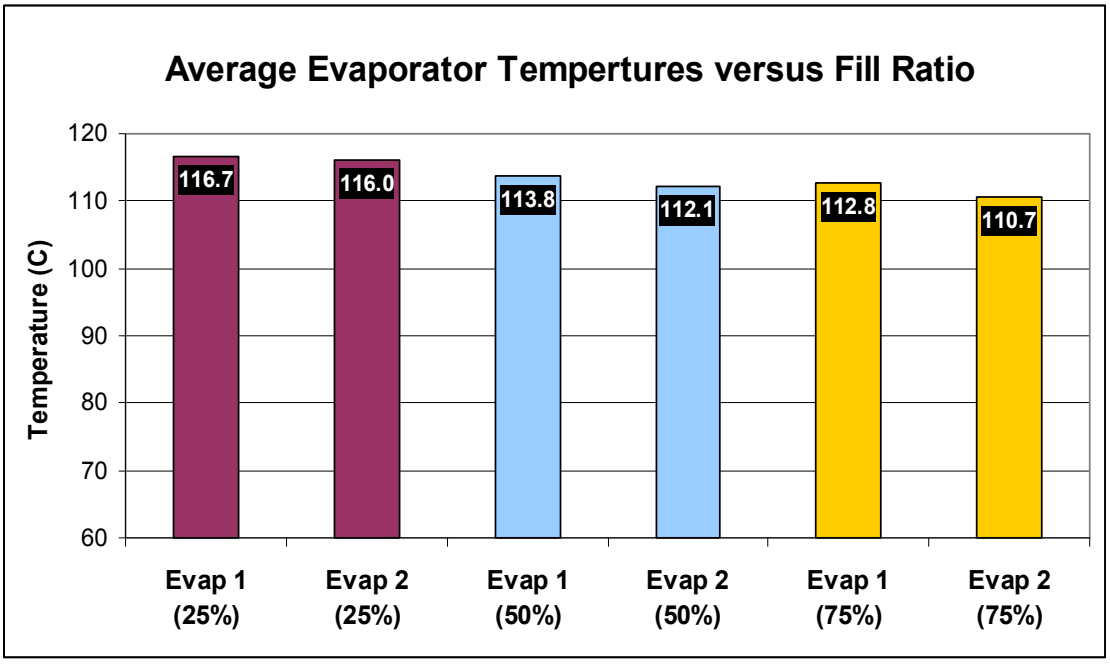

Figure 41: SLPHP Average Evaporator Temperature

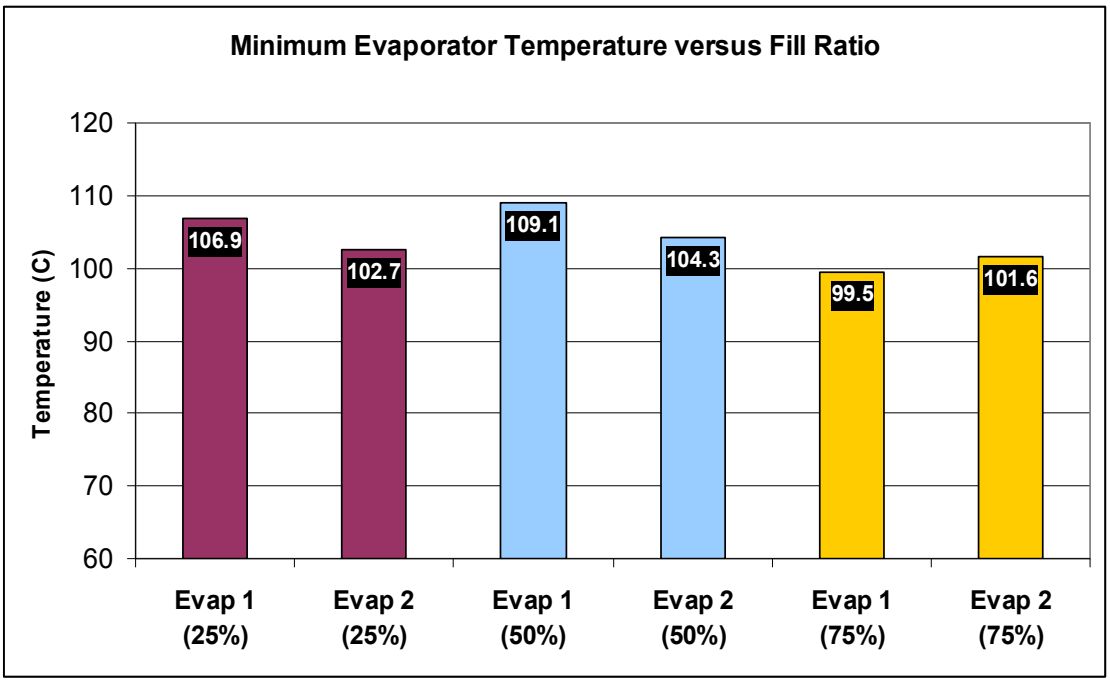

Figure 42: SLPHP Minimum Steady State Evaporator Temperature

In Figure 42 the trials using the 25% fill ratio attained an average minimum evaporator temperature of 104.8°C. An average minimum temperature of 106.7°C was observed during tests using 50% fill ratios, and an average of 100.5°C was observed for the system when a 75% working fluid fill ratio was observed. This temperature difference between the various trials may be due to an in the increase of the working fluid within the system. When compared with SLPHP devoid of working fluid, which attained an average evaporator temperature of 135 degrees Celsius, there seems to be some temperature regulation advantage given the working fluid fill ratio.

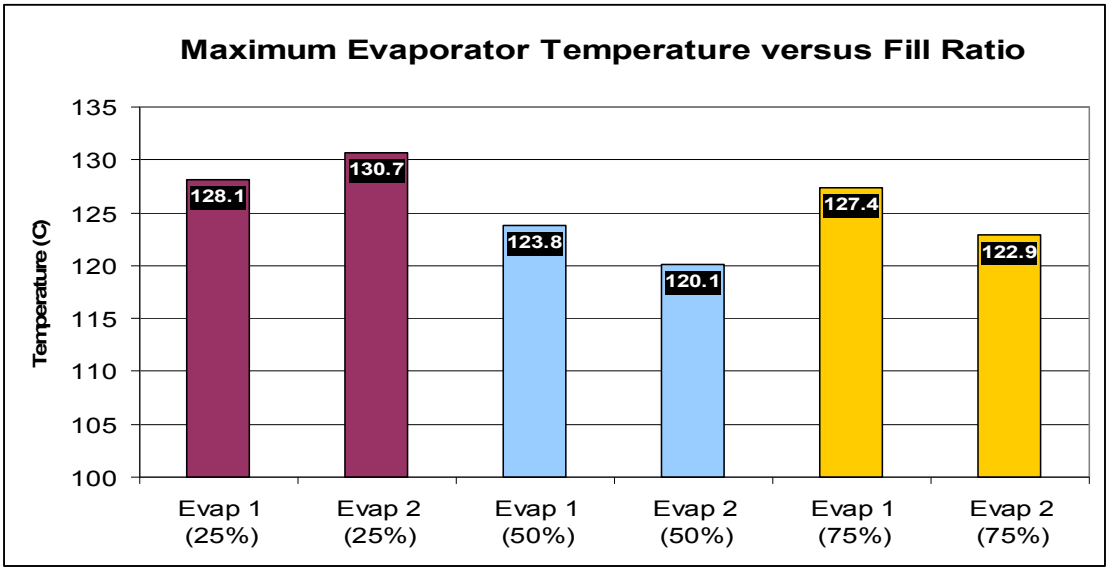

Figure 43: SLPHP Maximum Steady State Evaporator Temperature

As seen above in Figure 43 the maximum temperature of the SLPHP evaporator at steady state, across all fill ratio combinations was above 120°C. With the trials involving the 50% working fluid fill ratio attaining an average maximum average temperature of 121.95°C, which is much less than either the maximum temperatures attained by either 25% or 75% trials, meaning that the system was oscillating at a higher rate, allowing it to maintain the temperature range of the system much more effectively.

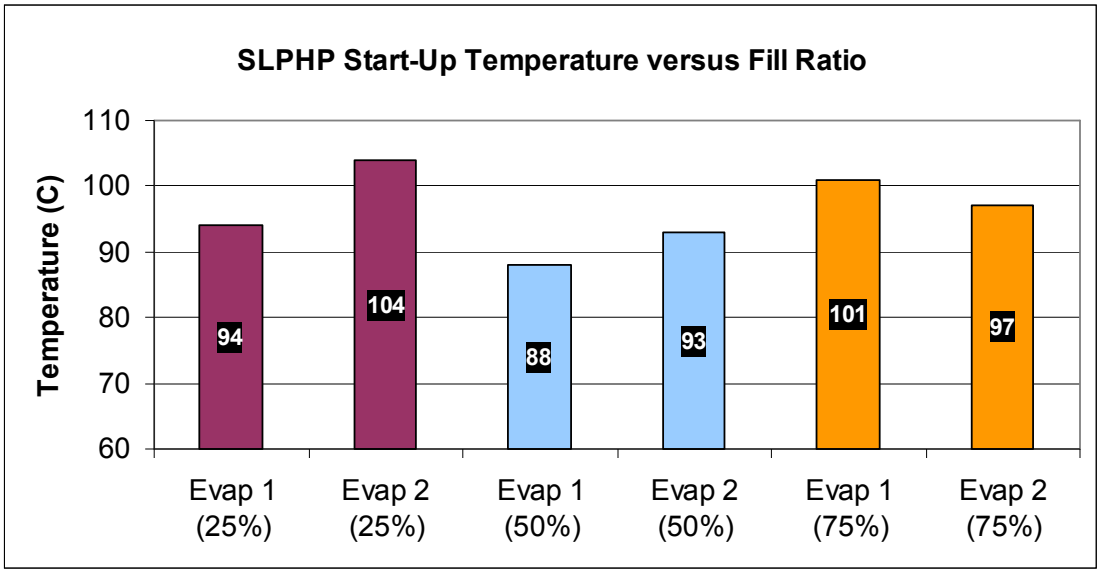

Figure 44: SLPHP Average Start-Up Temperature

The start-up temperatures, also referred to as the first point of temperature oscillation are displayed in Figure 44. The data was acquired from the experimental trials, which can be viewed in Figures 21, 22, 23, and 24. Trials involving a charge of 50% working fluid showed the first sign of temperature oscillation in the evaporator with an average temperature of 88°C and 93°C at various points on the tube structure respectively. The trials at 25%, however, experienced the first sign of temperature oscillation of 94°C and 104°C, and 101°C and 97°C for trials involving trials of 75% fill ratios.

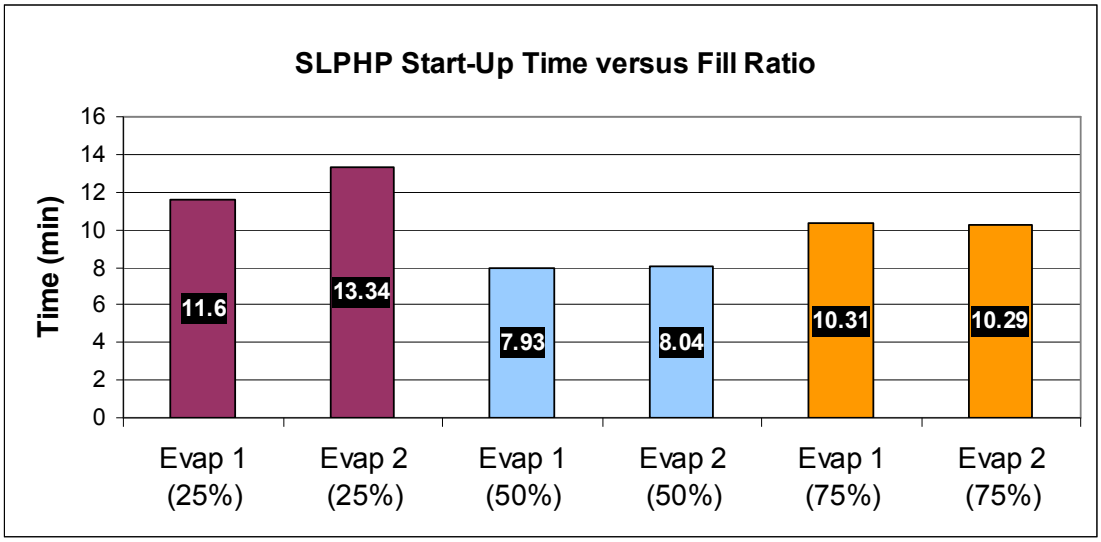

Figure 45: SLPHP Average Start-Up Time

The average start-up times of the SLPHP showed that the fill ratio had a significant effect on the time, in minutes, of when the system began to oscillate. Figure 45 shows that trials involving fill ratios of 50% displayed the shortest start-up time at an approximate average time of 8 minutes at first sight of oscillation. The next shortest start-up time involved trials at 75% fill ratio, with an average start up time of 10 minutes 15 seconds. The trials involving the system charged with 25% working fluid showed the slowest time with an average 12 minutes 28 seconds. It is to be understood that at the lower fill ratios, the vapor plugs produced are too large, and at lower temperatures, the pressure developed is not significant enough to warrant slug oscillation.

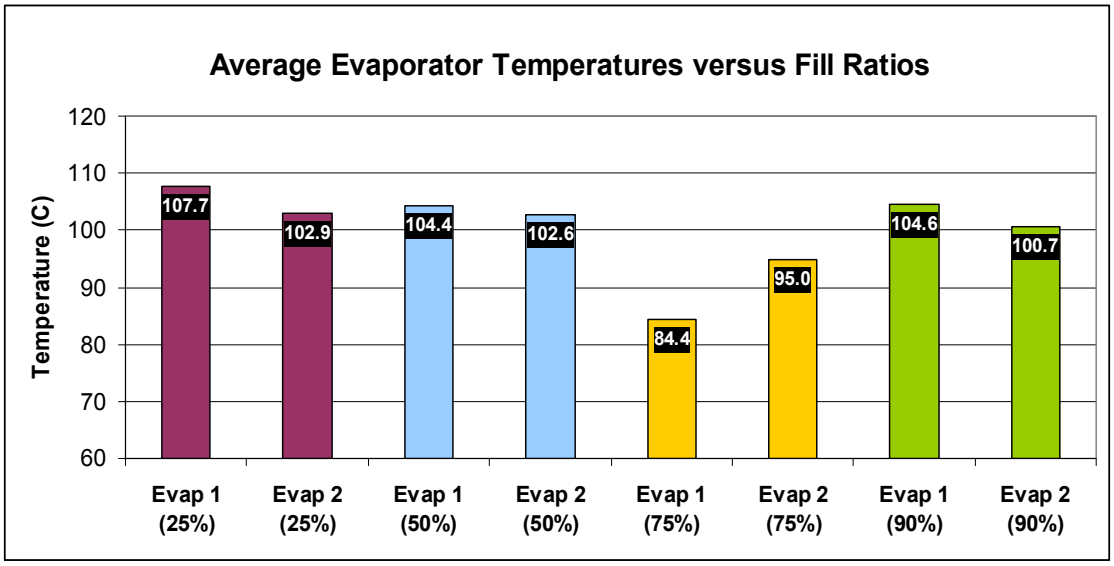

Figure 46: DLPHP Average Evaporator Temperature

The start-up temperatures, also referred to as the first point of temperature oscillation are displayed in Figure 46. The data was acquired from the experimental trials, which can be viewed in Figures 29, 30, 31, and 32. Trials involving a charge of 75% working fluid showed the first sign of temperature oscillation in the evaporator with an average temperature of 84.4°C and 95°C at various points on the tube structure respectively. Where as the trials at 25% experienced the first sign of temperature oscillation of 107°C and 102°C, and 104°C and 102°C for trials involving trials of 25% fill ratios. Trials involving a charge system of 90% showed similar start-up times to 25% and 50% trials, with average temperatures of 104°C and 100°C.

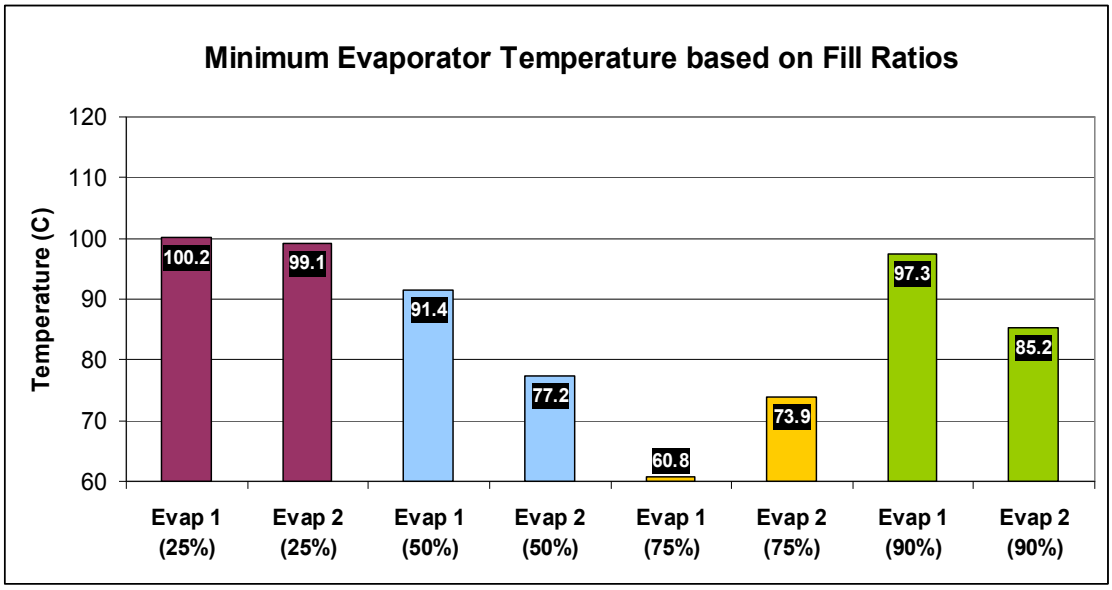

Figure 47: DLPHP Minimum Steady State Evaporator Temperature

In Figure 47 the trials using the 25% fill ratio attained an average minimum evaporator temperature of 99.65°C. An average minimum temperature of 84.3°C was observed during tests using 50% fill ratios, and an average of 67.35°C was observed for the system when a 75% working fluid fill ratio was observed, which shows strong pulsating flow between the evaporator and condenser. An average minimum temperature 96.25°C was observed with a charging working fluid ratio of 90%. This temperature difference between the various trials may be due to an increase of the working fluid within the system. When compared with DLPHP devoid of working fluid, which attained an average evaporator temperature of 130 degrees Celsius, there seems to be some temperature regulation advantage given the working fluid fill ratio.

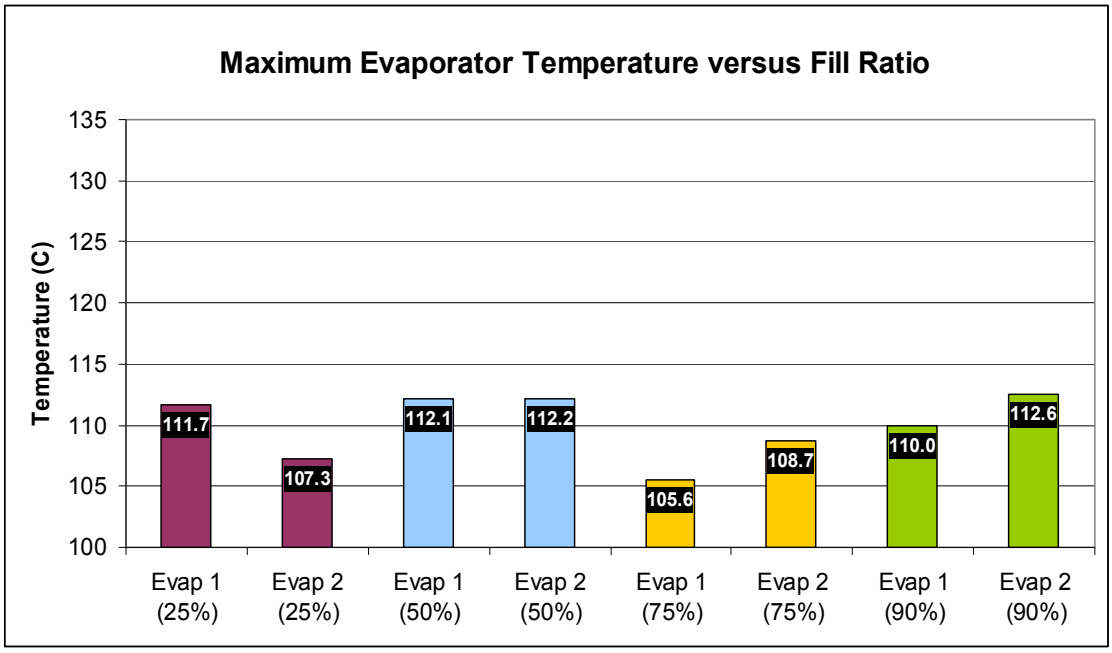

Figure 48: DLPHP Maximum Steady State Evaporator Temperature

The maximum evaporator temperature that is attained during a trial during steady state operation is another way to gauge the overall effective performance of a PHP, as discussed previously concerning the SLPHP. The maximum temperatures attained with the DLPHP configuration varied with dependence on the fill ratio of the working fluid, with the lowest maximum temperatures observed during trials involving fill ratios of 75% with average temperatures of 105.6°C and 108.7°C across the evaporator block. Fill ratios of 25%, 50%, and 90% showed similar average maximum temperatures, with an average of approximately 111°C.

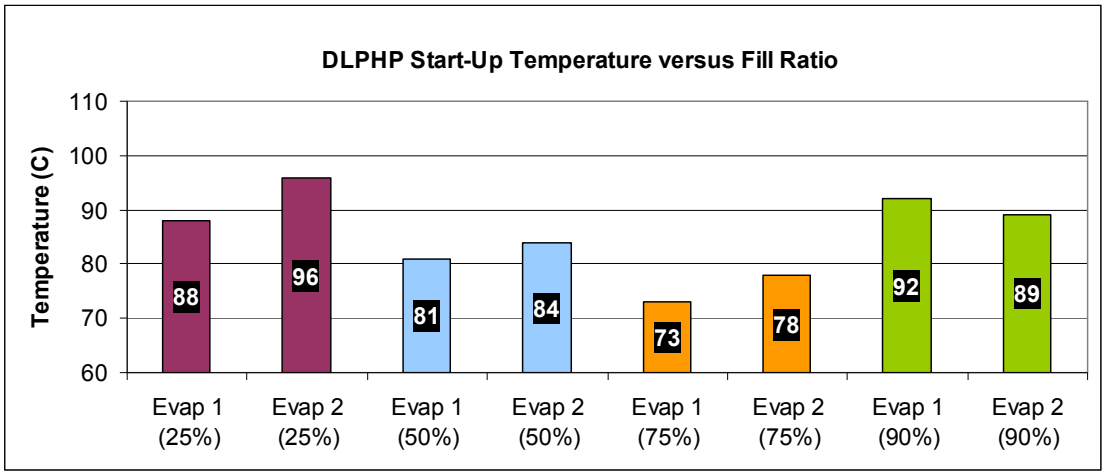

Figure 49: DLPHP Average Start-Up Temperature

As seen above in Figure 49 the start-up temperature of the DLPHP system varies substantially when each fill ratio experiment combination was analyzed jointly. The worst performance was attained using a charged fill ratio of 25% with an average start-up oscillation temperature of 92 degrees Celsius.

The next highest starting oscillation temperature involved a fill ratio of 90% with an average start-up temperature of 90 degrees Celsius. The quickest operating oscillation times were observed at both fill ratios of 50 and 75%, with an average temperature of 82.5 and 75.5 degrees Celsius respectively. The impact of the working fluid fill ratio and the beginning of operation is significant when comparing the difference between the 25% and 50% and 75% tests, with an average temperature difference of 10 degrees Celsius.

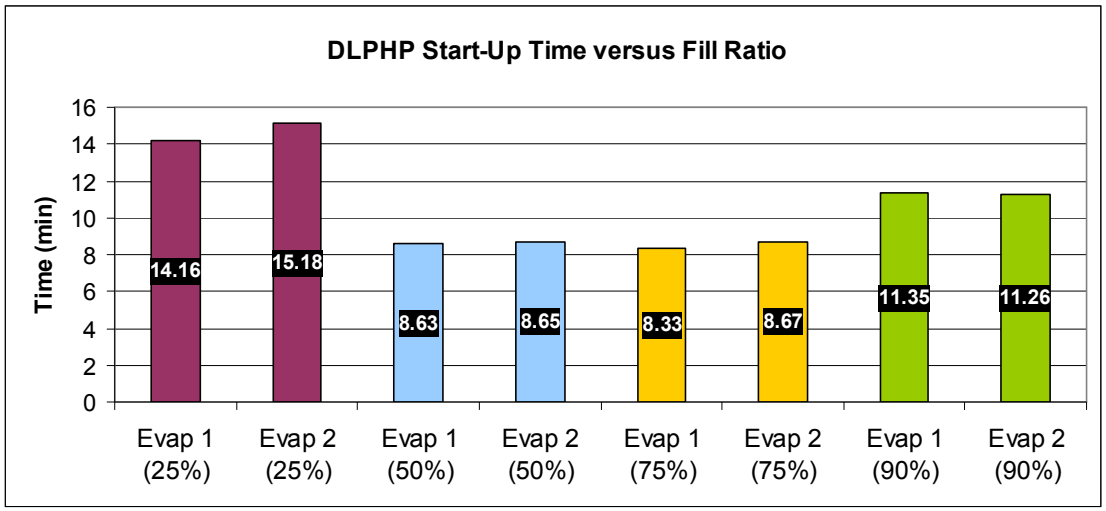

Figure 50: DLPHP Average Start-Up Time

As seen above in Figure 50 the start-up time of the DLPHP system varies substantially when each fill ratio combination is analyzed together. The worst performance attained using a fill ratio of 25% with an average start-up oscillation time of 14 – 15 minutes.

The next lowest performance fill ratio combination was experiments involving a fill ratio of 90% with an average start-up time of 11 ½ minutes. The quickest operating oscillation times were observed at both fill ratios of 50 and 75%, with an average time of 8 minutes and 40 seconds. The impact of the working fluid fill ratio and the beginning of operation is significant when comparing the difference between the 25% and 50% tests, with an average difference of 7 minutes.

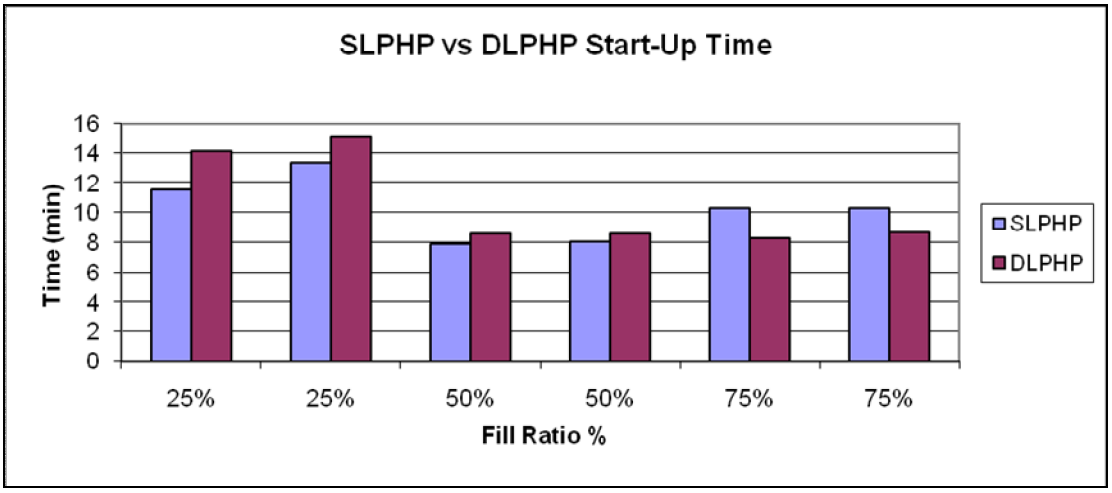

Figure 51: SLPHP vs. DLPHP Start-up Temperature

Figure 51, which displays the start-up time, also referred to as the first indication of temperature oscillation of the SLPHP and DLPHP evaporator, are compared side-by-side an interesting trend can be observed. The standard SLPHP appears to have a shorter start-up time, when the working fluid ratios are both 25% and 50%, which can be more apparent at the 25% fill ratio where there is an average difference of 2 minutes. This difference, while smaller, is still apparent when comparing the two systems at 50% fill ratio, with an average difference of 30 seconds. This tread reverses when the working fluid fill ratio is at 75%, where the evaporator temperature beings to fluctuate on average 2 minutes before the SLPHP.

A possible explanation for the faster start-up of the SLPHP at lower fill ratios may be due to an equal distribution of water and vapor slugs, and possible the friction of the working fluid upon the tube walls was smaller given the smaller volumetric geometry.

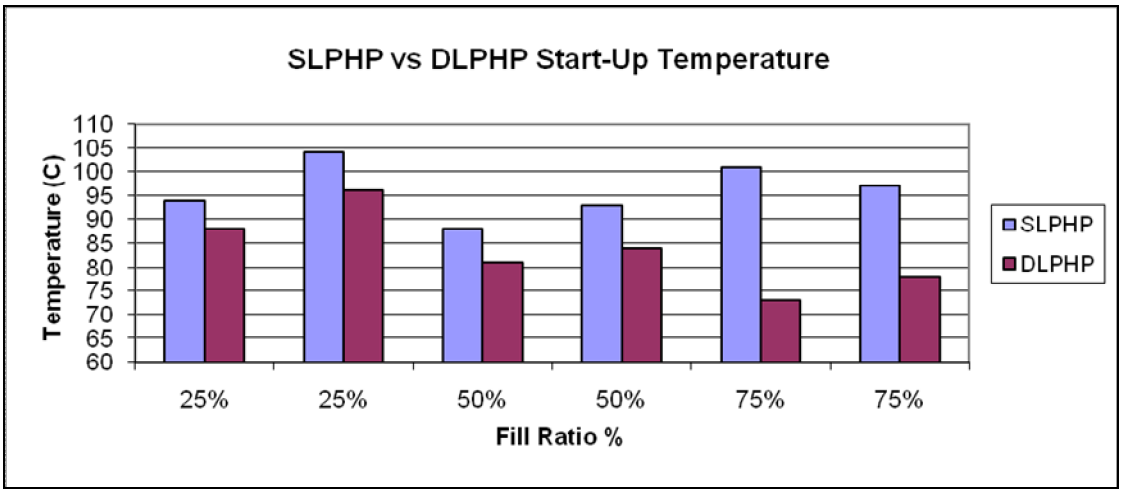

Figure 52: SLPHP vs. DLPHP Start-up Time

In contrast to the start-up oscillation time of the SLPHP and DLPHP, where the SLPHP took a shorter time for the system to begin to perform, the start-up temperature for when the systems began to oscillate is the opposite, which is evident in Figure 52. The SLPHP show a higher starting operational temperature then that of the DLPHP for all fill ratios. For tests involving charged ratios of 25%, the DLPHP began to oscillate 6-8 degrees Celsius earlier than a SLPHP with similar fill ratio. This tread continued when comparing the systems at 50% fill ratios with 5-7 degrees Celsius difference from the start-up temperatures of each system. The most significant difference was observed with a charge ratio of 75% which showed a 24-27 degree difference between the two systems.

SECTION 4.6 CHECK VALVE

A check-valve was added to the single layer pulsating heat pipe to observe its effect on the overall thermal performance of the system. Several experiments were conducted using different filling ratios as well as changing the orientation of the check valve itself to change the direction of flow of the working fluid. It was mentioned in several research articles that a check-valve would increase the overall thermal performance by regulating the direction of the fluid flow into one direction [7]. It was also mentioned in other research articles that a check-valve would actually be detrimental to the performance of the device [12]. The following experimental data and analysis was performed at two fill ratios, 75% and 90%. The check-valve, a SMC Spring Check Valve, 1/8 Inch MPT, of brass composition is of piston design, rated for 500 PSI, with a cracking pressure of 1 PSI, and was mounted along the outer most pipe, which can be seen in Figure 48.

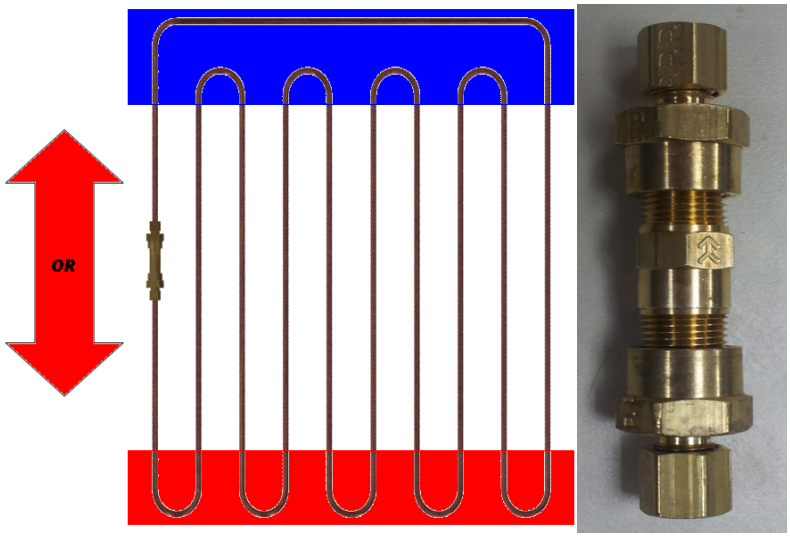

Figure 53: SLPHP with mounted Check-Valve

The experimental data was gathered in the same manner as the non-check-valve pulsating heat pipe system. The experimental data can be seen in the following figures

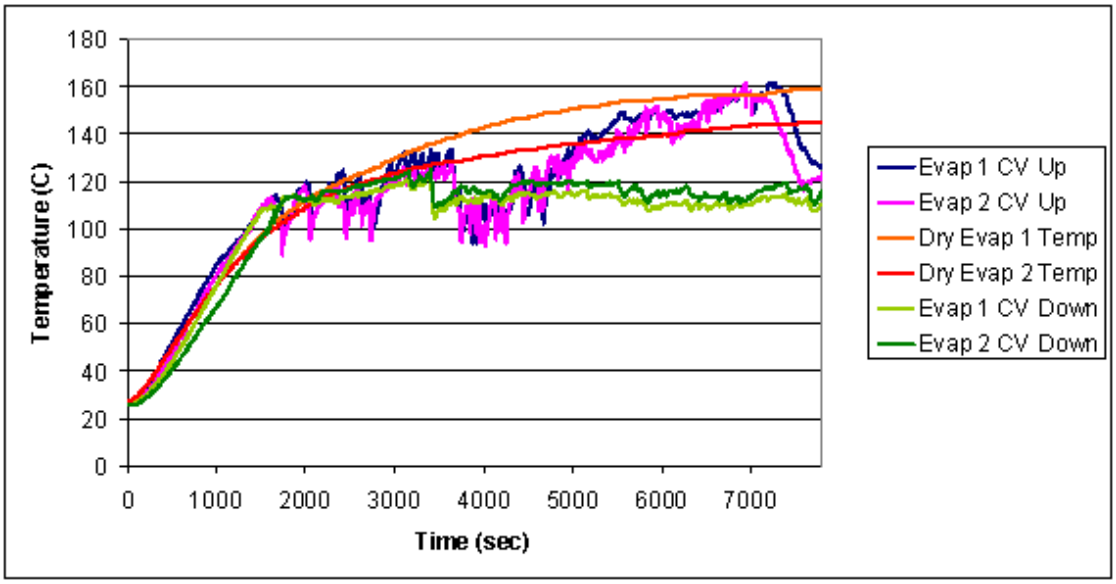

Figure 54: SLPHP with Check Valve: Up/Down Orientation at 75% Filling Ratio, and Dry

Figure 54 shows the experimental data compilation of the single layer pulsating heat pipe with a working fluid filling ratio of 75% as well as the system "dry" with no working fluid. Some interesting observations were noted, including the evaporator performance when the check-valve is in the "up" orientation, where high points of oscillation were present throughout the first half of the experiment (2000-4500 seconds) at a relative temperature range of 100-110 degrees Celsius. The second half of the experiment (4500 – 7500 seconds) showed an escalating temperature at both points along the evaporator which continued up to 160 degrees Celsius, or approximately 320 degrees Fahrenheit. It is hypothesized that the pulsating heat pipe is experiencing a "dry-out" scenario during this time frame, where the evaporator tubes are devoid of working fluid.

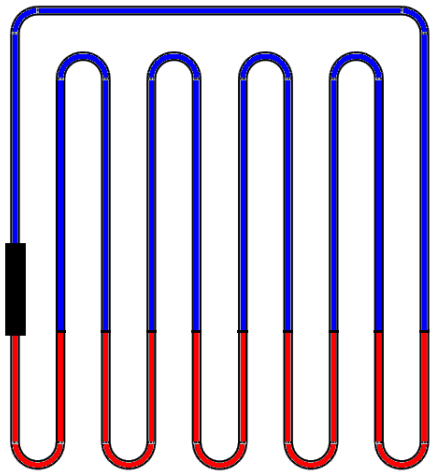

Figure 55: PHP with Check Valve – Dry Out Scenario – Red Region: Dry, Blue Region: Working Fluid

The "dry-out" scenario was not observed during, 75% filling ratio, trials not involving the check-valve. This potential cause of a "dry-out" may be from a restriction of the two-phase liquid/vapor oscillation flow. Using Figure 53, with the current location of the check valve and its flow direction facing "up" it may be assumed that the oscillating behavior was moving the liquid-vapor slugs/plugs through the check valve, with the vapor then condensing on the outlet. This would reduce the flow of the liquid through the upper condenser, as the condensed fluid would no longer be able to fall back down to the evaporator. This process leaves only vapor in the tubing attached to the inlet end of the check-valve, which would eventually lead to the increasing of undesirable temperatures and directly to a stagnation of the oscillating effect of the system, or "dry-out". The effect on the insulation, melting, from "dry-out" can be seen in Figure 55.

Another potential hypothesis is that the restricting flow of the check-valve and the effect of the filling ratio may have led a system operating in two different modes:

An oscillating mode, where half of the tube structures operate as a pulsating heat pipe and the other half operating as a pure conduction mode heat transfer device or a stagnant thermosyphon with “dry-out”. This hypothesis can be depicted in Figure 54.

Figure 56: SLPHP with Check-Valve – Up Orientation – 75% Filling Ratio – Dry-Out

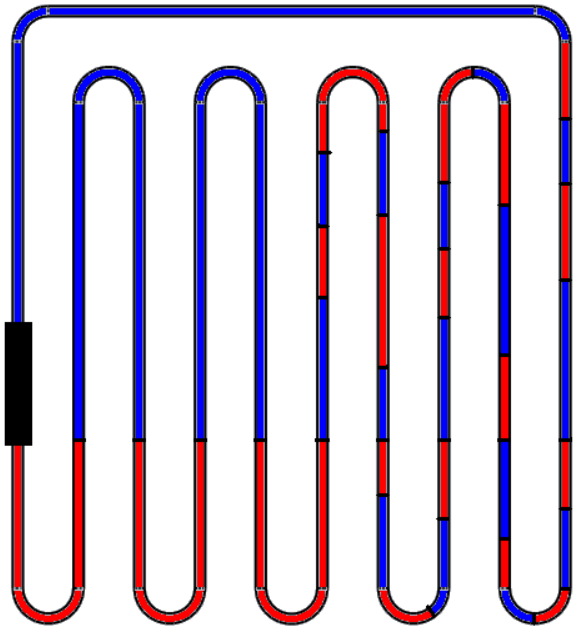

Figure 57: SLPHP with Check-Valve – Partial Operation – Half of System with Two-Phase Liquid/Vapor, other half, experiencing Dry-Out Scenario

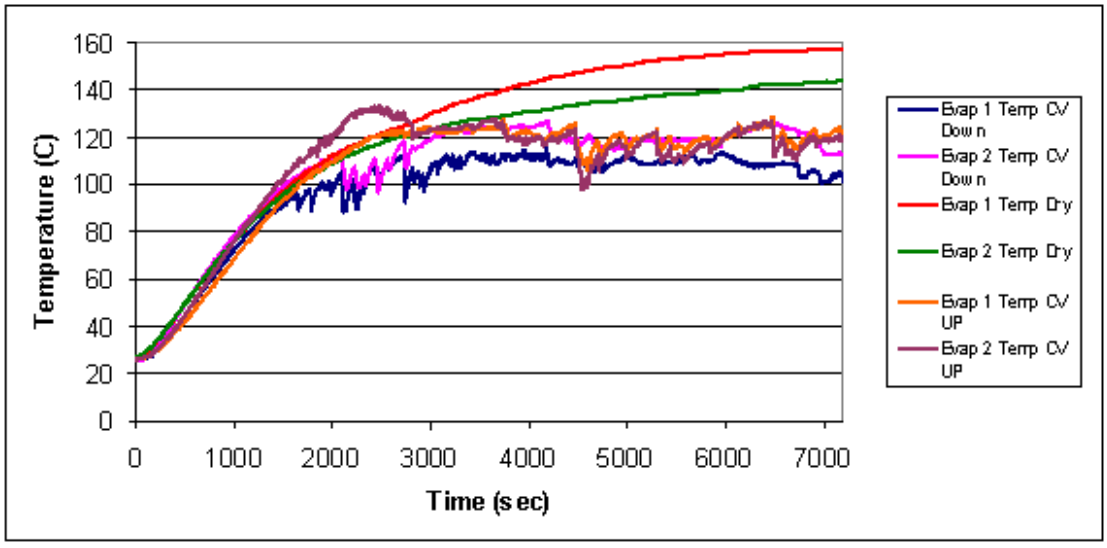

Figure 58: SLPHP with Check Valve: Up/Down Orientation at 90% Filling Ratio, and Dry

Figure 59: SLPHP with Check Valve: "Down" Orientation with 90% Filling Ratio

Figure 59 shows the adiabatic section with insulation sections damaged during an experimental trial involving a filling ratio of 90% with the check-valve in the "down" orientation, meaning the flow of the working fluid is directed toward the evaporator on the mounted tube section. In Figure 59 the evaporator is located on the bottom section of the figure, with the condenser located on top section of the figure.

The melting temperature of the above insulation is 82 degrees Celsius; using this information, it is assumed that locations of melted insulation indicated “dry-out” locations.

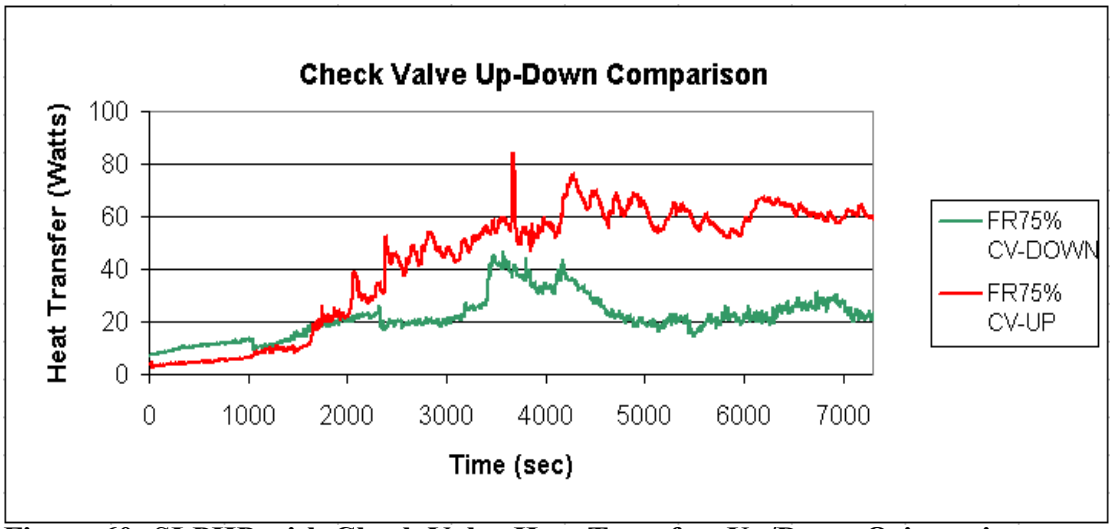

Figure 60: SLPHP with Check Valve Heat Transfer: Up/Down Orientation at 75% Filling Ratio

The heat transfer of each system was determined using the same methods which were mentioned with non-check valve systems. The results for each trial can be seen in Figures 60 and 61. From the analyzed preliminary data it appears the orientation of the check-valve has an impact on the over thermal performance of the pulsating heat pipe, with the check-valve in the “up” orientation showing the greatest performance for both the 75% and 90% filling ratio tests. The “up” orientation for the 75% filling ratio appeared to have a steady state operational heat transfer rate of 60 Watts, in the “down” orientation experiment a more sporadic heat transfer rate was observed, which appeared to have a running average of 22 Watts. The heat transfer performance of the system with a 90% filling ratio showed similar results between the two different orientation changes with an approximate performance of 25 watts. It seems that the filling ratio has still has an impact on the performance of the device,

similar to that of the pulsating heat pipe without a check valve, the reduction of the available vapor plugs, which are the driving force of the device, leads to a poor performing system. On the other hand the added working fluid reduces the chance of a "dry-out" scenario.

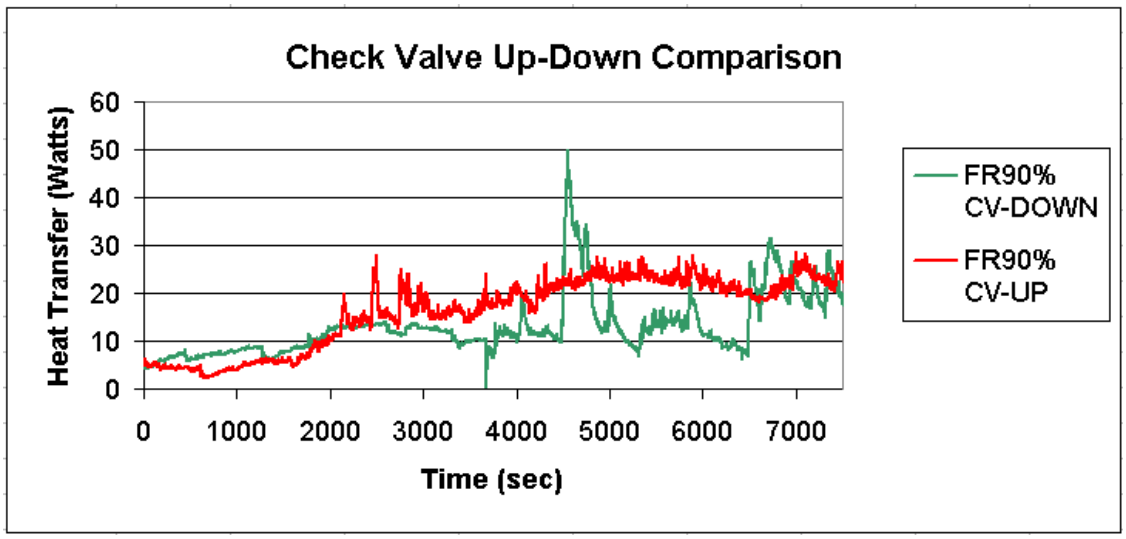

Figure 61: SLPHP with Check Valve Heat Transfer: Up/Down Orientation at 90% Filling Ratio

The preliminary data involving the orientation and location of the check-valve on a pulsating heat pipe shows much promise for further research. It seems apparent from the presented data that the orientation of the check valve has a significant impact on the behavior of the devise. Potential negative effects such as "dry-out" scenarios as well as the possibility of two-mode "dry-out" and "pulsating behavior" were observed. Further work can be performed in this area of research to see if the location of the check-valve will have a different effect.

CHAPTER 5

CONCLUSION

5.1 REVIEW

In review, an experimental analysis was undertaken to observe the characteristics and performance of a dual layer pulsating heat pipe when compared to a typical single layer pulsating heat pipe of similar construction given various dimensional constraints. To reiterate to what was previously discussed, a closed loop pulsating or oscillating heat pipe consists of a metallic tube of capillary dimensions bent in a serpentine manner and joined end to end. It is first evacuated and then filled partially with a working fluid, which then distributes itself naturally in the form of liquid-vapor slugs and bubbles inside the capillary tube [7], because of this, various sections of the tube structure have a different volumetric phase distribution. One end of the structure receives heat, which then transfers it to the other by a pulsating action of the liquid-vapor slug-plug system.

A DLPHP system is, in essence, the combination of two single layer pulsating heat pipes that have an interconnecting tube section, effectively placing them in a series orientation and allowing them to utilize the same working fluid. It was then assumed that given this interconnection the overall performance in thermal management and heat transfer characteristics would be increased more so than an independent traditional SLPHP exposed to the same heating and cooling sources.

Several characteristics of each device were observed, including the start-up temperature at which the working fluid begins to fluctuate, the temperature oscillation at various points in the evaporator section, the cooling bath exit temperature and the derived heat transfer calculations that were drawn from it. In addition, the thermal resistance of the overall system was determined, as well as the axial and radial heat flux of the evaporator block were calculated.

The assumption of a dual layer pulsating heat pipe was further developed by building off of previous research that determined that the efficiency of a pulsating heat pipe is dependent on the number of turn sections in respect to the inner diameter of the capillary tube structure being used which is determined experimentally. An in-plane pulsating heat pipe's efficiency can be increased by horizontally extending the system with additional bends and turns.

While applying this thought process and application to industry one can potentially run into some limitations. If a metallic tube structure is used, composed of copper or steel, there is a certain physical minimum bend radius that can be achieved in relation to the inner and outer diameters of the tube, before an undesirable crimp or defect appears. Given this information, the overall dimensional footprint of the device would be dependent upon the minimum bend of the tube structure.

Given a certain dimensional footprint of the heating element, the number of overall bends that can fit said dimensions can be determined, and as stated previously the efficiency of a pulsating heat pipe is dependent on a high number of turns. The thermal management, performance, and application, of a PHP can be significantly

hampered if the critical number of tubes cannot be achieved given the dimensional constraint.

It was concluded that the dual layer system outperformed the single layer system in many aspects throughout the testing regime, even though each tube structure embedded within the evaporator received half of the heat flux in respect to those of the SLPHP. The DLPHP attained an overall lower thermal resistance at steady state operation in respect to various fill ratios, with a minimum thermal resistance value of 0.12 °C/W when compared to the thermal resistance calculated from the SLPHP which was approximately a minimum value of 0.85 °C/W.

The DLPHP was also able to transfer more heat per the given watt density of the evaporator block when compared to the SLPHP at various fill ratios. At steady state operation the DLPHP, at a fill ratio of 75%, was able to transfer heat of an average 105 Watts to the condenser cooling fluid, which would be an apparent operating efficiency of 87.5%. When compared to the SLPHP at its most efficient fill ratio of 50% attained a maximum heat transfer of 55W to the cooling fluid for an overall efficiency of approximately 45%.

The evaporator was also maintained at a lower temperature with the DLPHP then what was attained by the SLPHP at all fill ratio tests. The average temperature at the DLPHP most efficient fill ratio of 75% was approximately 80 degrees Celsius, with minimum temperatures of 62 degrees Celsius attained during some tests; this is significant when compared to data gathered from the SLPHP, which experienced a relative consistent evaporator temperature of 110 degrees Celsius through all fill ratio tests. Both of these conclusions are significant when compared to the system devoid of

working fluid where the evaporator maintained an average temperature of 160 degrees Celsius.

It can be concluded from an experimental investigation that interconnecting pulsating heat pipes of equal geometry and over laying them on a given restricted dimensional heat source with a given power input and heat flux, performs better than an independent pulsating heat pipes of equal geometry in the same configuration.

5.2 FUTURE WORK

Further work may be performed involving pulsating heat pipes that may also further improve their potential use in real world applications. One path of research would be to develop an active pump within the tube structure that would be constructed out of a memory foam material that would change shape or move when a heat is applied to it. This is similar to a check valve that also regulates the flow of the working flow of the system, except a check valve is a passive instrument that relies on the system to move the fluid through it. A pump, which utilizes the temperature developed by the system and actually moves the fluid itself would be much more beneficial and possibly improve the overall performance of the system. Another such research opportunity would possibly be a system that reuses the transferred heat and power from the PHP system and turns it into electrical power, possibly creating regenerative electrical properties that may help reduce the power consumption of a device or extend the usage time of a mobile device, such a laptop computer by partially recharging the battery.

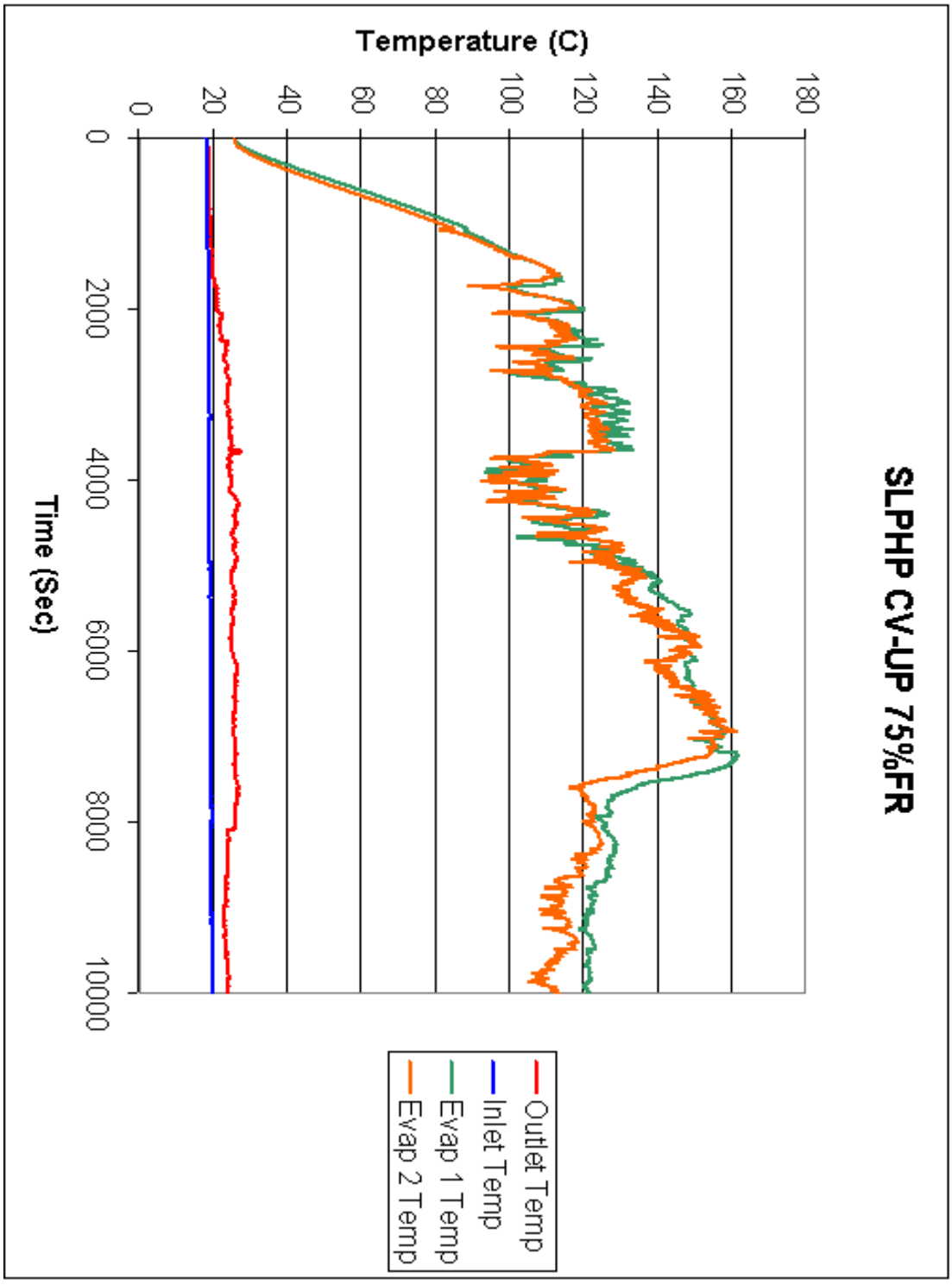
SLPHP CV-UP 75%FR
Temperature (C)
180
160
140
120
100
80
60
40
20
0
0
2000
4000
6000
8000
10000
Time (Sec)
Outlet Temp
Inlet Temp
Evap 1 Temp
Evap 2 Temp

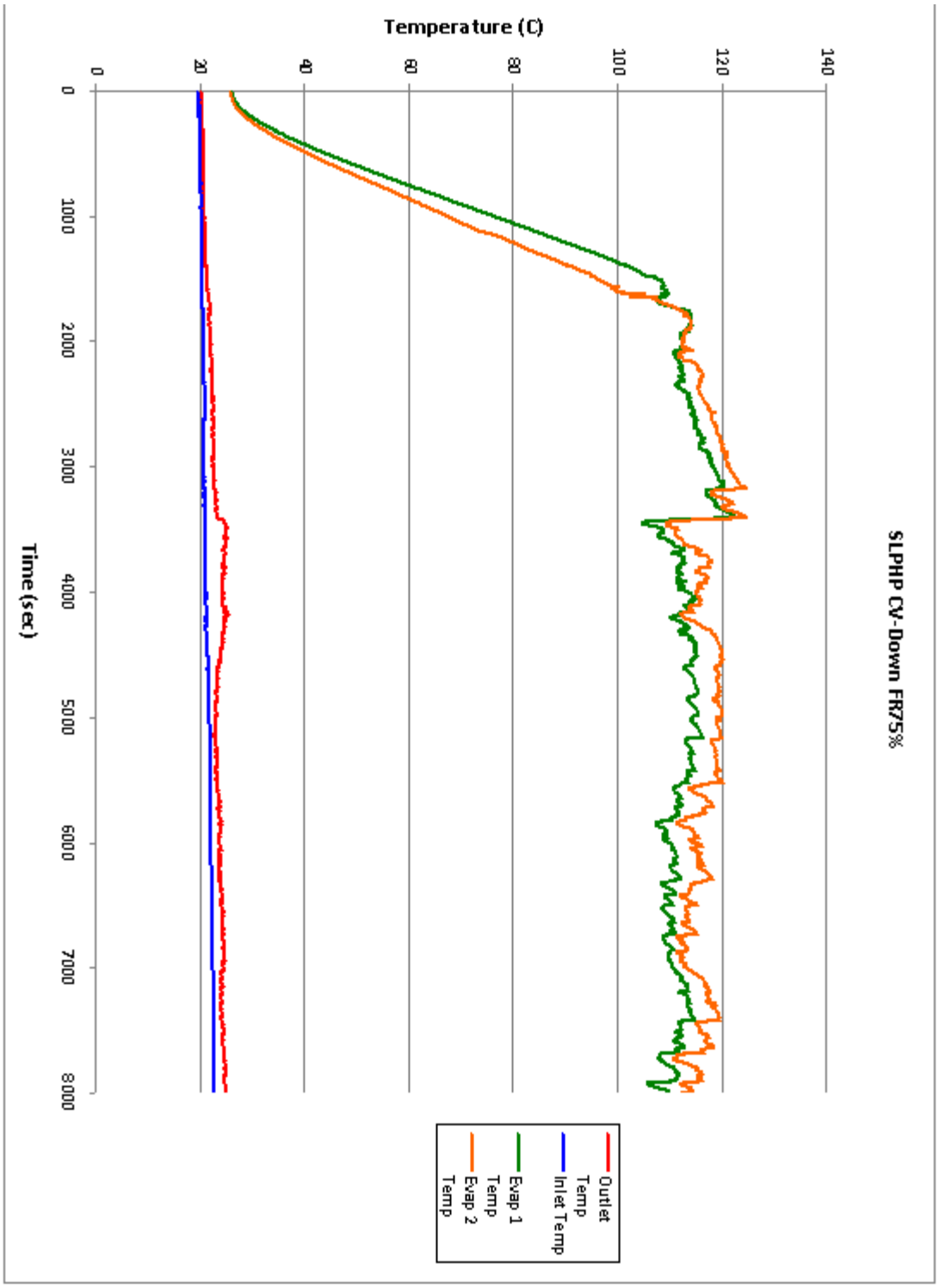
SLPHP CV-Down FR75%
Temperature (C)
Time (sec)
0
20
40
60
80
100
120
140
0
1000
2000
3000
4000
5000
6000
7000
8000
Outlet Temp
Inlet Temp
Evap 1 Temp
Evap 2 Temp

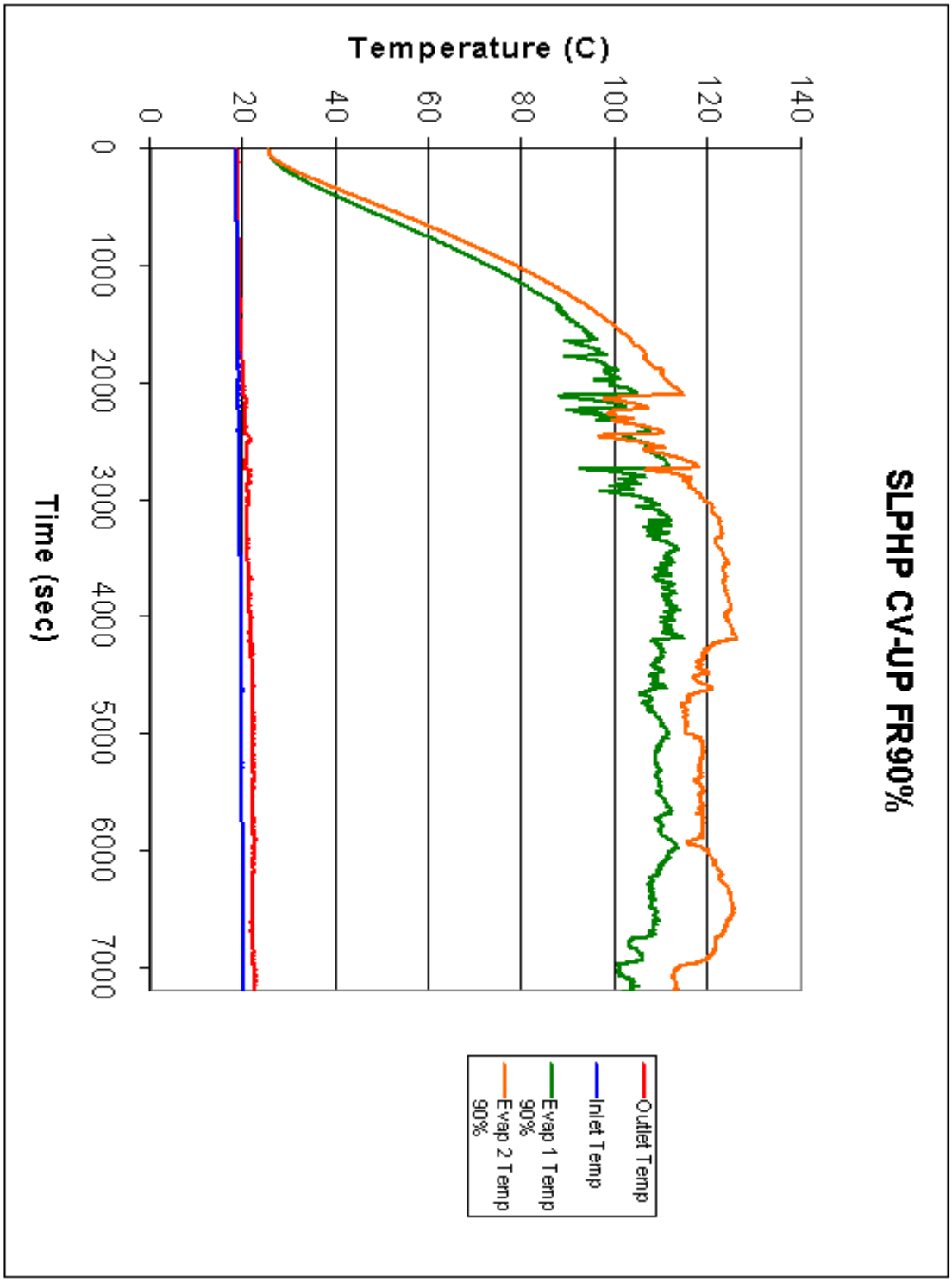
SLPHP CV-UP FR90%
Temperature (C)
140
120
100
80
60
40
20
0
0
1000
2000
3000
4000
5000
6000
7000
Time (sec)
Outlet Temp
Inlet Temp
Evap 1 Temp 90%
Evap 2 Temp 90%

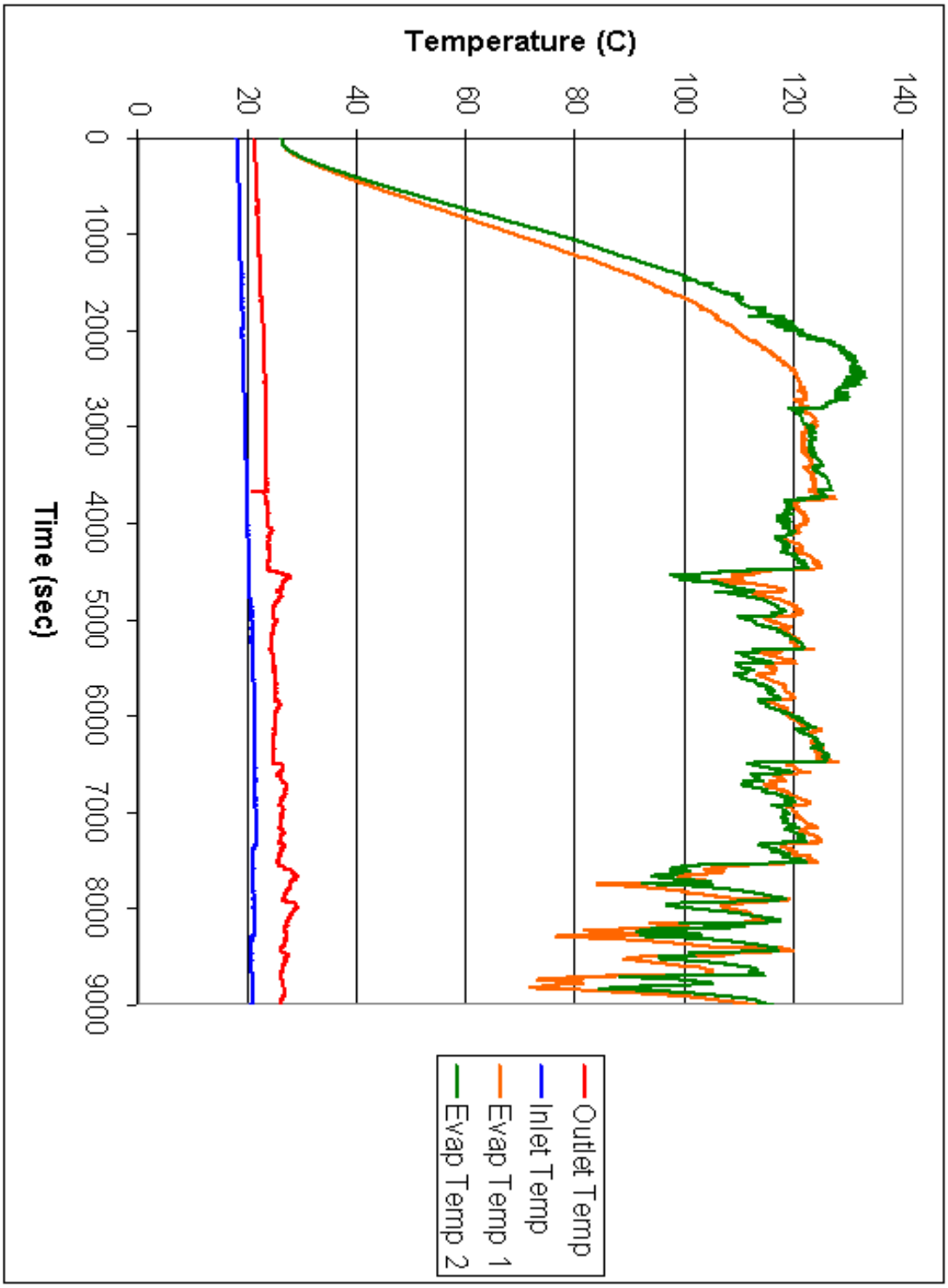
Temperature (C)
140
120
100
80
60
40
20
0
0
1000
2000
3000
4000
5000
6000
7000
8000
9000
Time (sec)
Outlet Temp
Inlet Temp
Evap Temp 1
Evap Temp 2

BIBLIOGRAPHY

Akachi, H., 1990, "Structure of a Heat Pipe", US Patent, No. 4,921,041.

Gilver C. R and Martinez J. M. Modeling of Pulsating Heat Pipes Sandia National Laboratories, Albuquerque, New Mexico, 2009.

Incropera Frank P., DeWitt David P., Bergman Theodore L., Lavine Adrienne. Fundamentals of Heat and Mass Transfer 6th Edition. *Chapter 11: Heat Exchangers*. John Wiley & Sons, 2007.

Khandekar, S., M. Schneider, P. Schafer, R. Kulenovic, and M. Groll, *Thermofluid dynamic study of flat-plate closed-loop pulsating heat pipes*, Microscale Thermophysical Engineering, 2002.

Khandekar, S., Gupta A. *Embedded Pulsating Heat Pipe Radiators*. 14th International Heat Pipe Conference, Florianopolis, Brazil, April 22-27, 2007.

Karimi G., Culham J.R. *Review and Assessment of Pulsating Heat Pipe Mechanism for High Heat Flux Electronic Cooling*, Inter-Society Conference on Thermal Phenomena 2005, pg 52-58.

Moran Michael, J., Shapiro Howard, N. Fundamentals of Engineering Thermodynamics 6th Edition, *Chapter 10: Refrigeration and Heat Pump Systems.* John Wiley & Sons, Inc. 2008.

Qu, W. and HB Ma, *Theoretical Analysis of start-up of a pulsating Heat Pipe*, International Journal of Heat and Mass Transfer, 2007.

White Frank M. Fluid Mechanics 6th Edition. *Chapter 6: Viscous Flow in Ducts*. The McGraw-Hill Companies, Inc. 2008.

Zhang, Y., A. Faghri, *Heat transfer in a pulsating heat pipe with open end*, International Journal of Heat and Mass Transfer, 2002, 775-764.

Zhang, Y., A. Faghri, *Oscillatory Flow in Pulsating Heat Pipes with Arbitrary Numbers of Turns*, Journal of Thermophysics and Heat Transfer Vol. 17, No. 3, July-September 2003.

REFERENCES:

[1] Gilver C. R and Martinez J. M. Modeling of Pulsating Heat Pipes Sandia National Laboratories, Albuquerque, New Mexico, 2009.

[2] Qu, W. and HB Ma, *Theoretical Analysis of start-up of a pulsating Heat Pipe*, International Journal of Heat and Mass Transfer, 2007.

[3] Zhang, Y., A. Faghri, *Heat transfer in a pulsating heat pipe with open end*, International Journal of Heat and Mass Transfer, 2002, 775-764.

[4] Zhang, Y., A. Faghri, *Oscillatory Flow in Pulsating Heat Pipes with Arbitrary Numbers of Turns*, Journal of Thermophysics and Heat Transfer Vol. 17, No. 3, July-September 2003.

[5] Khandekar, S., M. Schneider, P. Schafer, R. Kulenovic, and M. Groll, *Thermofluid dynamic study of flat-plate closed-loop pulsating heat pipes*, Microscale Thermophysical Engineering, 2002.

[6] Khandekar, S., Gupta A. *Embedded Pulsating Heat Pipe Radiators*. 14th International Heat Pipe Conference, Florianopolis, Brazil, April 22-27, 2007.

[7] Karimi G., Culham J.R. *Review and Assessment of Pulsating Heat Pipe Mechanism for High Heat Flux Electronic Cooling*, Inter-Society Conference on Thermal Phenomena 2005, pg 52-58.

[8] Akachi, H., 1990, "Structure of a Heat Pipe", US Patent, No. 4,921,041

[9] Moran Michael, J., Shapiro Howard, N. Fundamentals of Engineering Thermodynamics 6th Edition, *Chapter 10: Refrigeration and Heat Pump Systems.* John Wiley & Sons, Inc. 2008.

[10] Incropera Frank P., DeWitt David P., Bergman Theodore L., Lavine Adrienne. Fundamentals of Heat and Mass Transfer 6th Edition. *Chapter 11: Heat Exchangers*. John Wiley & Sons, 2007.

[11] White Frank M. Fluid Mechanics 6th Edition. *Chapter 6: Viscous Flow in Ducts*. The McGraw-Hill Companies, Inc. 2008.